ANALYSIS OF THE DEVELOPMENT OF THE MESSOYAKHA GAS FIELD:

A COMMERCIAL GAS HYDRATE RESERVOIR

A Thesis

by

ROMAN YURYEVICH OMELCHENKO

Submitted to the Office of Graduate Studies of
Texas A&M University
in partial fulfillment of the requirements for the degree of

MASTER OF SCIENCE

Approved by:

Chair of Committee,	Ahmad Ghassemi
Committee Members,	Walter Ayers
	Maria Barrufet
Head of Department,	Dan Hill

December 2012

Major Subject: Petroleum Engineering

ABSTRACT

Natural gas is an important energy source that contributes up to 25% of the total US energy reserves (DOE 2011). An increase in natural gas demand spurs further development of unconventional resources, including methane hydrate (Rajnauth 2012). Natural gas from methane hydrate has the potential to play a major role in ensuring adequate future energy supplies in the US. The worldwide volume of gas in the hydrate state has been estimated to be approximately 1.5 x 10^{16} m^3 (Makogon 1984). More than 230 gas-hydrate deposits have been discovered globally. Several production technologies have been tested; however, the development of the Messoyakha field in the west Siberian basin is the only successful commercial gas-hydrate field to date.

Although the presence of gas hydrates in the Messoyakha field was not a certainty, this current study determined the undeniable presence of gas hydrates in the reservoir. This study uses four models of the Messoyakha field structure and reservoir conditions and examines them based on the available geologic and engineering data. CMG STARS and IMEX software packages were used to calculate gas production from a hydrate-bearing formation on a field scale. Results of this analysis confirm the presence of gas hydrates in the Messoyakha field and also determine the volume of hydrates in place. The cumulative production from the field on January, 1 2012 is 12.9 x 10^9 m^3, and it was determined in this study that 5.4 x 10^9 m^3 was obtained from hydrates.

The important issue of pressure-support mechanisms in developing a gas hydrate reservoir was also addressed in this study. Pressure-support mechanisms were investigated using different evaluation methods such as the use of gas-injection well

patterns and gas/water injection using isothermal and non-isothermal simulators. Several aquifer models were examined. Simulation results showed that pressure support due to aquifer activity was not possible. Furthermore, it was shown that the water obtained from hydrates was not produced and remained in the reservoir. Results obtained from the aquifer models were confirmed by the actual water production from the field. It was shown that water from hydrates is a very strong pressure-support mechanism. Water not only remained in the reservoir, but it formed a thick water-saturated layer between the free-gas and gas-hydrate zone.

Finally, thermodynamic behavior of gas hydrate decomposition was studied. Possible areas of hydrate preservation were determined. It was shown that the central top portion of the field preserved most of hydrates due to temperature reduction of hydrate decomposition.

DEDICATION

This work is dedicated to my family, relatives and friends. My mom and dad have been supportive, loving, and patient throughout this process. My relatives have always been overly supportive and proud of my academic endeavors - I am blessed and grateful.

ACKNOWLEDGEMENTS

Author is obliged to Texas A&M University for the opportunity to carry research and present this work. I would like to express my gratitude to my advisor, Dr. Ahmad Ghassemi, his support and encouragement. I wish to thank my committee members, Dr. Walter Ayers and Dr. Maria Barrufet for giving me useful comments. I would very much like to recognize the input of Dr. Yuri F. Makogon for sharing his excellent insight on hydrate fundamentals, directing my work and his critical assessment of the obtained results. I also would like to thank Seth Podhoretz for his time and help in preparing the work.

NOMENCLATURE

KV1, KV2, KV3, KV4, KV5 = coefficients for equilibrium K value calculations

rxk1, rxk2, rxk3, rxk4, rxk5 = correlation coefficients

CPG1-4 are the gas heat capcity coefficients

CPL1-4 - are the liquid heat capcity coefficients

CT1-2 = thermal expansion coefficients

visg = gas viscosity

a_p, a_{gr} = coefficients of thermal conductivity of the solution and soil

C_p = specific heat of solution

ρ_P = density of the solution

K = coefficient of thermal conductivity

m_1 = mass of the gas released from hydrates decomposition per unit time

V_1 = volume of fluid in the borehole

β = the ratio of the coefficients of heat transfer of gas and liquid,

q_1 = the amount of heat per unit volume of gas (heat of decomposition of hydrates transferred into the well stream gas evolved)

m_2 = mass of evaporated methanol at given P and T

q_2 = latent heat of vaporization of methanol minus the specific heat of solution gas in methanol

V_2 = volume of liquid in contact with the gas

ΔT_{sk} = the temperature change in the time

T_P = temperature of the solution in the well during the 3d step

R = radius of the well

r = variable, the distance from the well axe to any point in the wellbore

d_{gr} = heat exchange coefficient of soil and wellbore

t_1 = time of gas hydrate decomposition of mass m_1

T = current time interval

OGIP = Initial gas in place

A = area

h= height

B_g = gas formation volume factor

S_w = water saturation

G_p = cumulative gas produced

G = original gas in place

Z = z –factor

P = pressure

T = temperature

i = index – initial

VRR = volume replenishment ratio

SWAG – simultaneous water and gas injection

TABLE OF CONTENTS

LIST OF FIGURES

Page

LIST OF TABLES

Page

CHAPTER I

INTRODUCTION AND LITERATURE REVIEW

1.1. Brief overview of the history of gas hydrates

It has been 47 years since the article, “The formation of hydrates in gas-bearing reservoirs" was published in the Gas Industry Journal № 5, 1965, and 43 years since the Messoyakha gas hydrate field development began (Makogon 1965). The potential world resources of gas hydrates are conservatively estimated to be 1.5×10^{16} m^3 (5.29×10^{17} SCF). More than 230 gas hydrate deposits have been discovered around the world, and several production technologies have been tested. However, the development of Messoyakha field is the only example of a successful commercial gas hydrate project.

On numerous occasions, it has been suggested that natural gas hydrates could exist in pipelines (Hammerschmidt 1934) and beneath the surface. In 1943, one of the first scientists to propose hydrate formation was Donald Katz, a professor at the University of Michigan. His hypothesis was based on oilfield and gas field development data in northern Canada. However, he failed to scientifically prove hydrate existence (Makogon 1997). The second attempt at suggesting the existence of natural gas hydrates was made by professor Strizhev in 1946 (Gubkin Russian State University of Oil and Gas) (Makogon 1997). He also expressed skepticism about the feasibility of developing gas hydrate fields.

Throughout the 1950s, the USSR rapidly expanded its gas industry and encountered major problems associated with the formation of hydrates in the transportation systems. These problems resulted in the increasing study of hydrate formation and decomposition conditions (Makogon 1965).

While drilling an exploratory well in the Markha River field (Yakutiya, Russia) in 1963, a gas blowout occurred, which gradually subsided. Using data obtained during the drilling, it was determined that gas at these pressures and temperatures could only exist in the hydrate state (Makogon 1965). With mixed reaction from the scientific community, additional research was required to prove the existence of gas hydrates.

Elaborate research was performed in 1965 and 1966 to study the formation and decomposition conditions of hydrates in porous media, including testing of real cores. The results obtained under specific pressures and temperatures confirmed that hydrates can be formed in porous media. The results of this work were presented at the Conference of Young Professionals and Scientists (Moscow 1965). After international examination of this work, the results were registered in the State Register as a scientific discovery in the USSR, No.75 (December 24, 1969).

Only 48 papers of pure academic studies on hydrates were published during the period ranging from 1778 to 1934. The results of approximately 151 studies were published between 1934 and 1965, and after the discovery of natural gas hydrates (Makogon 1965), the number of papers published increased significantly to 12,000. The Markha River field and not the Messoyakha field is the first discovery of a gas hydrate field. However, the Messoyakha field is the first commercial application of hydrate development and shows the potential of this vast resource.

Results of laboratory studies and the first data from the Messoyakha gas hydrate field development were presented at the XI International Gas Congress and the VIII International Petroleum Conference (Makogon 1997). These presentations attracted enormous interest among international engineers and scientists in the petroleum industry.

Several countries have initiated their own federal gas hydrate research programs following the Messoyakha first field development data that was reported in 1971. More than 150 wells have been drilled and thousands of kilometers of seismic and core sampling have been collected. Several production methods have been tested in Canada, the USA, and Japan; however, commercial development has been achieved only in the Messoyakha field.

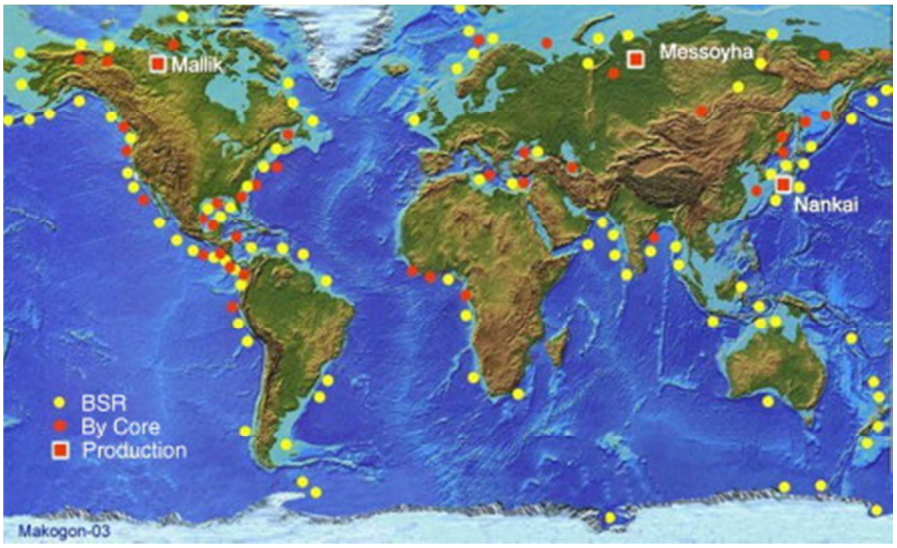

Figure 1 - Known gas hydrate deposits (identified by bottom simulating reflector, core sampling, and direct production) (Makogon 1997)

1.2. Gas hydrates as a potential source of energy

Natural gas is an important energy source that makes up to 25% of the total US energy consumption (DOE 2011). An increase in natural gas demand increases the need to identify different types of unconventional resources, including gas hydrates. Natural gas from methane hydrates has the potential to play a major role in ensuring adequate

future energy supplies in the US. The worldwide volume of gas in the hydrate state has been estimated to be in the range of $1.5*10^{16}$ m^3 ($53*10^{16}$ SCF) (Makogon 1984).

Gas hydrates are solid substances made of gas and water molecules that exist under conditions of high pressures and low temperatures. Hydrates are crystalline solids, very similar to ice, wherein hydrate-forming molecules are trapped inside cages of water molecules with hydrogen bounds. Hydrate-forming substances are usually low-molecular weight gases such as methane, ethane, and propane. Hydrates are formed wherever suitable conditions of temperature and pressure exist. Methane hydrates occur generally in Arctic regions and in ocean floor sediments (Fig. 1). Naturally occurring hydrates are mainly methane hydrates, due to the availability of low-molecular weight natural gas in the subsurface. Methane hydrates are receiving increased attention from engineers and scientists because of their high-energy density and resource potential. One unit volume of methane hydrate releases as much of 164 unit volumes of natural gas after dissociation.

Methane hydrates have been the subject of active research in the oil and gas industry since the discovery of hydrate plugging of oil and gas transportation systems (Hammerschmidt 1934). Makogon proposed that natural gas hydrates could exist in the earth's subsurface (Makogon 1965). One volume of water during hydrate formation binds 207 volumes of methane, and 1 volume of methane hydrate contains 164.6 volumes of free methane at standard conditions (Fig.2).

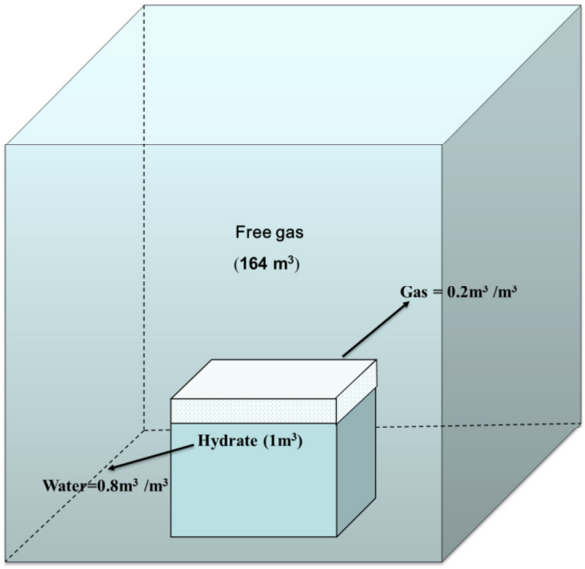

Figure 2 - Methane hydrate composition (Makogon 1966)

According to the estimates (Table 1), approximately 1.5 x 10^{16} m^3 (53 x 10^{16} SCF) of methane is trapped in a hydrate state (Makogon 1984). Approximately 97% of methane hydrates are in sediments under the sea floor's surface. The total gas resources in gas hydrates are two orders of magnitude greater than the total amount of methane in conventional reservoirs of the world.

Such a high potential of gas resources has prompted many countries to initiate R&D programs in the field of natural gas hydrate exploration and production.

Table 1 - Estimates of In-Situ MHs (Sloan 2008).

Year	CH_4 amount, 10^{15} m^3	Citation
1973/1977	3053/1135	Trofimuk et al.
2010	15	Makogon
1985	1573	Cherskiy et al.
1981	3.1	McIver
1988/1999	18/21	Kvenvolden
2000	0.2	Soloviev, Ginsburg

Active development and implementation work is now underway in many countries, including Japan, the USA, Canada, India, China, and Korea. As a result, significant achievements have been made in the exploration and development of gas hydrate reservoirs.

1.3. Review of the current state of gas hydrates R&D projects and resources development in Canada, Japan, the USA, and India

Japan achieved the greatest success in gas hydrate research. Since 1995, active research and development has been carried out to evaluate the resource potential and various commercial ways to assess opportunities for gas production from the Nankai offshore gas hydrate deposit (Fig. 3) Seismic surveys conducted between 1996 and 1997 revealed a widespread BSR (bottom simulating reflector) at a TVD (total vertical depth) of 1240 m (4067 ft) (290 m (952 ft) below the sea floor). The temperature field has shown that the BSR line at a given depth corresponds to the zone of hydrate stability (Matsumoto 2002).

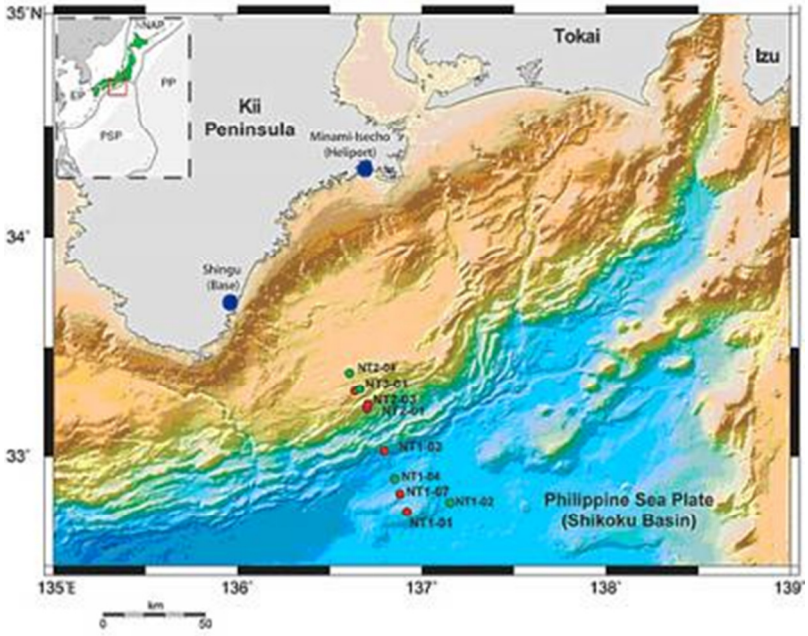

Figure 3 - Nankai gas hydrate field

Two major Japanese companies JNOC (Japan National Oil Company) and JPEX (Japan Petroleum Exploration Company) with the participation of GSC (Geological Survey of Canada) and the USGS (United States Geological Survey) organized a joint scientific research project in 1998 to carry out field tests in Mackenzie Delta (Canada). High-gas hydrate saturation as well as some geological and geochemical properties of the hydrate deposits at the Mallik site (Canada) (Fig. 4) is similar to those in the Nankai hydrate field (Japan).

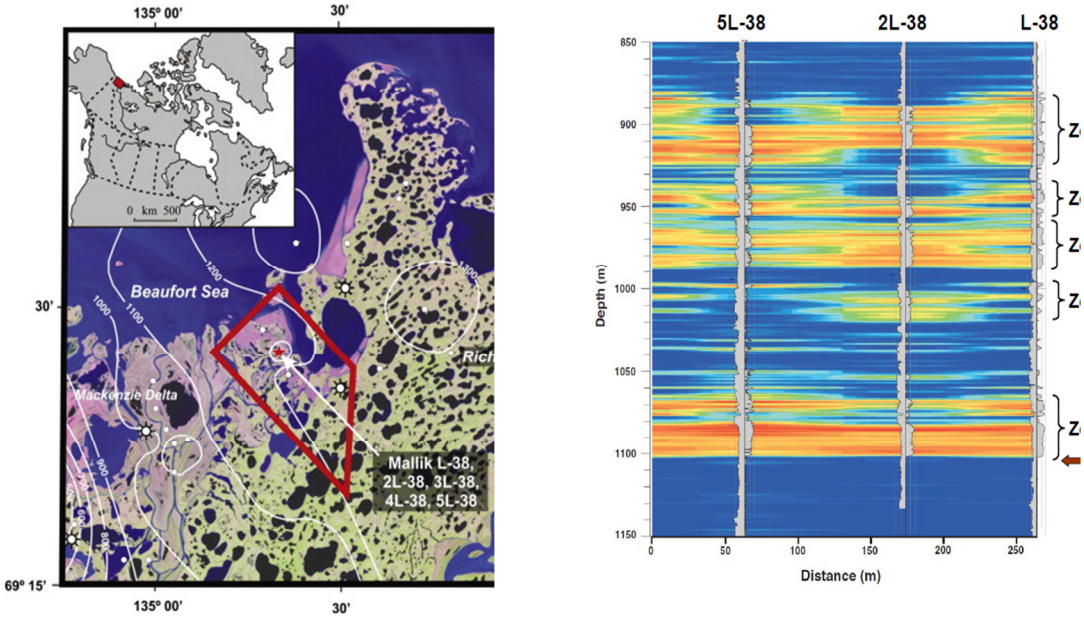

Figure 4 - a) Mackenzie river, northwest Canada, b) fence diagram showing well log-derived gas hydrate concentrations for Mallik research program wells

The experimental well Mallik 2L - 38 was drilled in 39 days and completed in March 1998. The well was drilled to a TVD of 1150 m (3,775 ft) with continuous coring. A total of 37 m (120 ft) of core samples were recovered from the interval of 886 to 952.6 m (2,905 to 3,125 ft). The Mallik L-38 well revealed at least 10 gas hydrate formations at depths between 810.1 and 1102.3 m (2,655 and 3,615 ft). The permafrost zone thickness was 640 m (2,100 ft) in the area (Kurihara et al. 2010).

As a result of these studies, the porosity and hydrate saturation distribution was obtained in the hydrate-saturated intervals. Average porosity was 30%, and the hydrate saturation varied from 0 to 90%. Hydrate-saturated intervals were identified the depths of 888.84 to 1101.09 m (2,915 to 3,610 ft). 1.5 m (5 ft), and a thick free gas layer was detected below the hydrate intervals.

The density of gas resources in hydrates obtained from the well was 4.15 billion m^3/km^2 (380 BSCF/sq. mile). The OGIP (original gas in place) at

the Mallik site was estimated to be on the order of 110 billion m^3 (3.8 TSCF) (Collet 2002). Based on the experience gained during the research of the Mallik 2L-38 well, JAPEX and JNOC began a drilling program in the Nankai trough, offshore Japan.

Six exploration wells were drilled from a semisubmersible platform in 1999 and 2000. The drilling site was 50 km (31 miles) south of the Shizuoka Prefecture (Honshu) where the most distinct BSR (bottom simulator reflector) was observed on the seismic profiles. Geophysical surveys and core samples confirmed the presence of at least three hydrate reservoirs with total thicknesses of 16 m (53 ft) at a TVD of 1135 to 1213 m (3,725 to 3,980 ft). The total volume of gas trapped in the hydrate state is equivalent to 756 million m^3 of gas per km^2 (69 BSCF/sq. mile). Based on the results obtained, the total resources in the region are estimated to be 4.13 to 20.64 $x10^9$ m^3 (145 to 728 BSCF), which at current projections could secure an energy supply for Japan in excess of 50 years (Schebetov 2008).

The North Slope of Alaska is one of the most promising gas hydrate region in the US (Tabatabaie and Pooladi-Darvish 2012). The presence of hydrates was confirmed with an exploration well drilled at the Prudhoe Bay field in 1972. Additional interpretation of the well logs from 51 well sites revealed a gas hydrate reservoir. The Prudhoe Bay - Kuparuk River area has six distinct hydrate reservoirs, four of which are in hydrodynamic contact with the underlying free gas (Fig. 5). Hydrate saturation and porosity for individual layers is 85% and 42%, respectively.

ConocoPhillips with Anchorage AK Japan Oil, Gas, and Metals National Corporation (JOGMEC) conducted a trial production technology test based on carbon dioxide (CO_2) injection during the winter and spring of 2012 (Schoderbek 2011). The

goal of this project was to test a new technology for methane hydrate production in which CO_2 molecules are exchanged in situ for methane (CH_4) molecules in a hydrate structure, releasing methane gas for production. The objectives of the production technology test were to evaluate the viability of this hydrate production technique and to understand the implications of the process at a field scale (Collett et al. 2012).

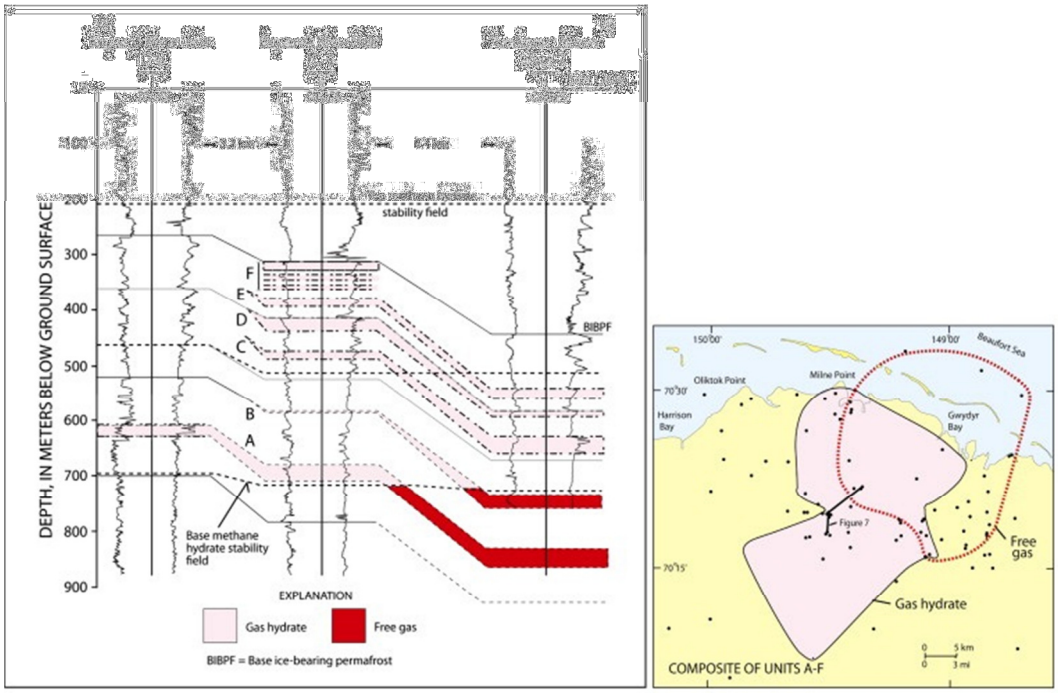

Figure 5 - (a) Cross section showing the lateral and vertical extent of gas hydrates and underlying free-gas occurrences in the Prudhoe Bay-Kuparuk River area in northern Alaska (Collett 1992)

The OGIP trapped in hydrates is estimated to range from 1.0 to 1.2 trillion m^3 (35 to 42 TSCF), which is nearly twice the gas reserves the free state at the Prudhoe Bay field (Collett 1992).

In addition to the North Slope of Alaska, some gas hydrate deposits were discovered on the east coast of the US at Blake Ridge (Makogon 2010). Several seismic

surveys and 11 wells drilled in the area revealed 26 km^2 (10 sq. miles) of gas hydrate accumulations at ocean depths ranging from 1 to 4 km (0.62 to 2.48 miles). A seismic line through Well #994, 995, and 997 is shown in Fig. 6.

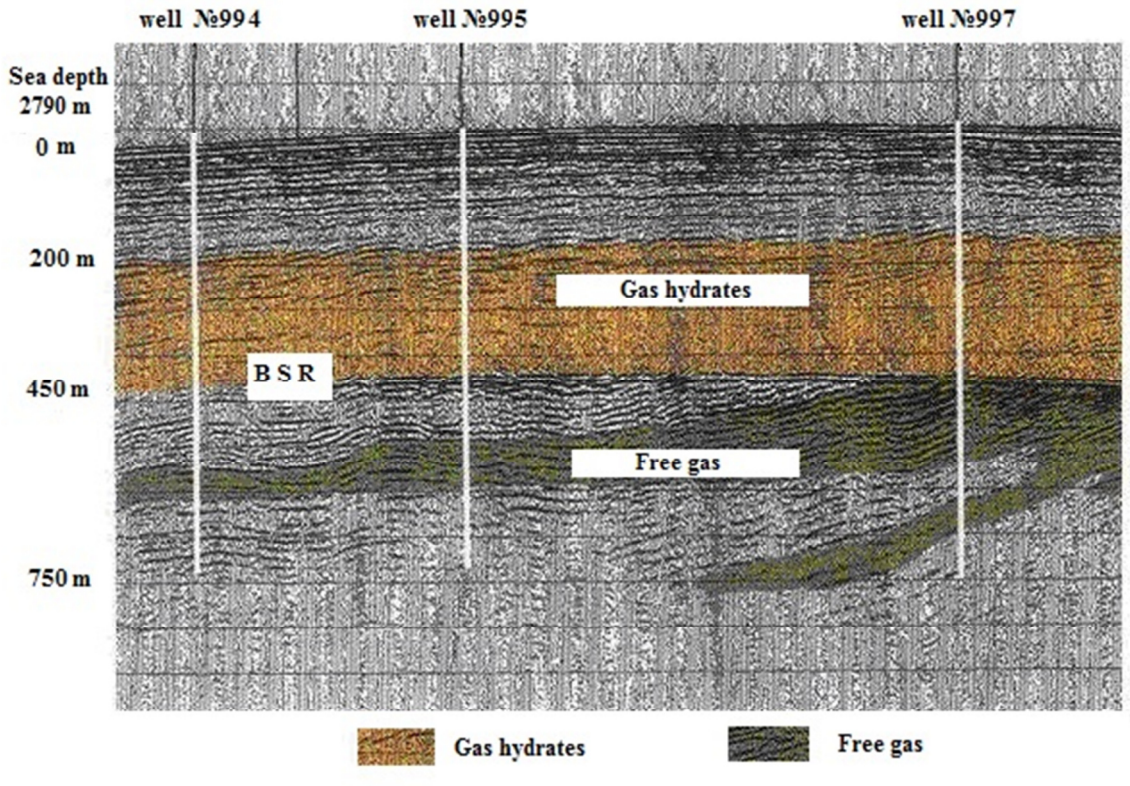

Figure 6 – Seismic line from Blake Ridge reservoir showing locations of the Well #997, 994, and 995 (Makogon 2010)

Well #997 penetrated nine gas hydrate-bearing layers extending from 203 to 434 m. The net thickness varies from 10 to 360 cm (0.328 to 12 ft) with an average net thickness of 7.5 m (25 ft). The average porosity is 57%. Gas hydrate saturation is between 3 and 12%. A 125-m (410-ft) thick free-gas layer was identified immediately below the BSR at a TVD of 3216 m (10,550 ft). Porosity of the gas-saturated interval is 53%. Gas resources in the region range from 25 to 411 x 10^6 m^3/km^2 (2.285 to 37.55

BSCF/sq. mile). Total resources of gas for the Blake Ridge are approximately 57 x 10^9 m^3 (2.11 TSCF).

The Gulf of Mexico is another well-known area containing gas hydrates (Manohar Gaddipati 2012). Several research projects have been performed to study the hydrate accumulations in the Gulf of Mexico. The high interest in hydrates in this area is due to their potential threat to the conventional oil and gas offshore construction methods. Gas hydrate dissociation in the Gulf of Mexico leads to wellbore and seabed instability.

As part of the Indian National Program, hydrate studies were carried out on the continental shelf of India. According to the calculations made by the National Institute of Oceanography, the hydrate stability zone has an average thickness of 200 to 400 m (656 to 1,312 ft) (in some areas, greater than 800 m (2,625 ft)) at a water depth ranging from 600 to 3000 m (2,000 to 10,000 ft). The BSR line was found in the area 140,000 km^2 (53,800 sq. miles) in the eastern shelf of India in the Krishna-Godavari basin. Seven potential areas were identified in the Andaman basin at a TVD extending from 850 to 2000 m (2,800 to 6,560 ft). The Bay of Bengal and Mahanadi river deltas and the Krishna-Godavari region are notable potential regions. According to estimates, the total gas resources in the hydrate state are approximately 1,894x 10^9 m^3 (66 TSCF), which is 1,900 times greater than conventional gas reserves in India. Even the production of 1% of these gas resources can provide the entire country over the next several decades (Jha et al. 2012).

1.4. Overview of production technologies of gas from gas hydrates

The basic principle of gas production from hydrates in a reservoir with an impermeable cap is the transformation of hydrates from solid state to a free-gas state, which is produced by conventional methods. A need exists for the development of methods that will improve the gas hydrate decomposition efficiency. There are three methods to decompose gas hydrates (Fig. 7):

- Lower the reservoir pressure below the equilibrium pressure (depressurization) out of the hydrate stability zone as represented by curve 1 (Fig.7);
- Increase the reservoir temperature above the equilibrium temperature out of the hydrate stability zone as represented by the curve 2 (Fig.7);
- Inject chemicals that change the equilibrium conditions for hydrate formations (position of the blue solid line) or form more preferable hydrates in the pores (CO_2).

The proper choice of the development technology of gas hydrate deposits depends on the specific geological and physical conditions, especially the degree of "overcooling" (the difference between the reservoir temperature and equilibrium).

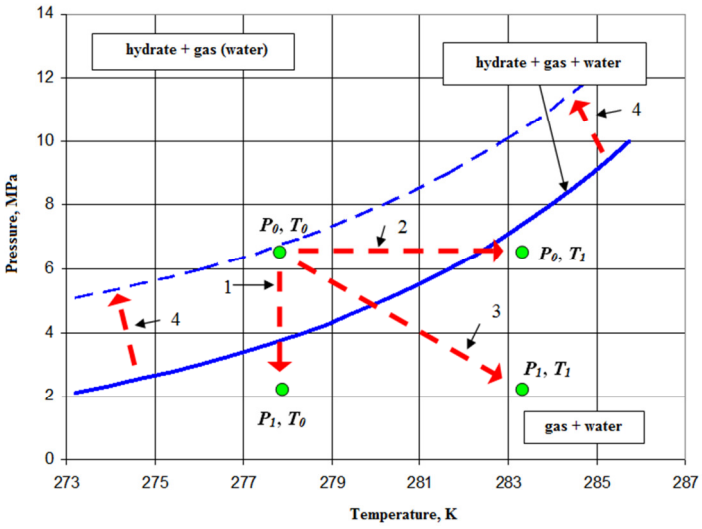

Figure 7 - Methods of gas hydrate production: 1) depressurization; 2) thermal stimulation; 3) chemicals injections

For example, the development of a gas hydrate reservoir with a small net pay having an impermeable lithologic layers and low-permeability rocks at the boundary of GWC (gas-water contact), with a slight overcooling of hydrate reservoir, should be based on lowering the reservoir pressure below the equilibrium and producing free gas and water by conventional methods (Fig.8) because of low-drawdown pressure required for decomposition initiation.

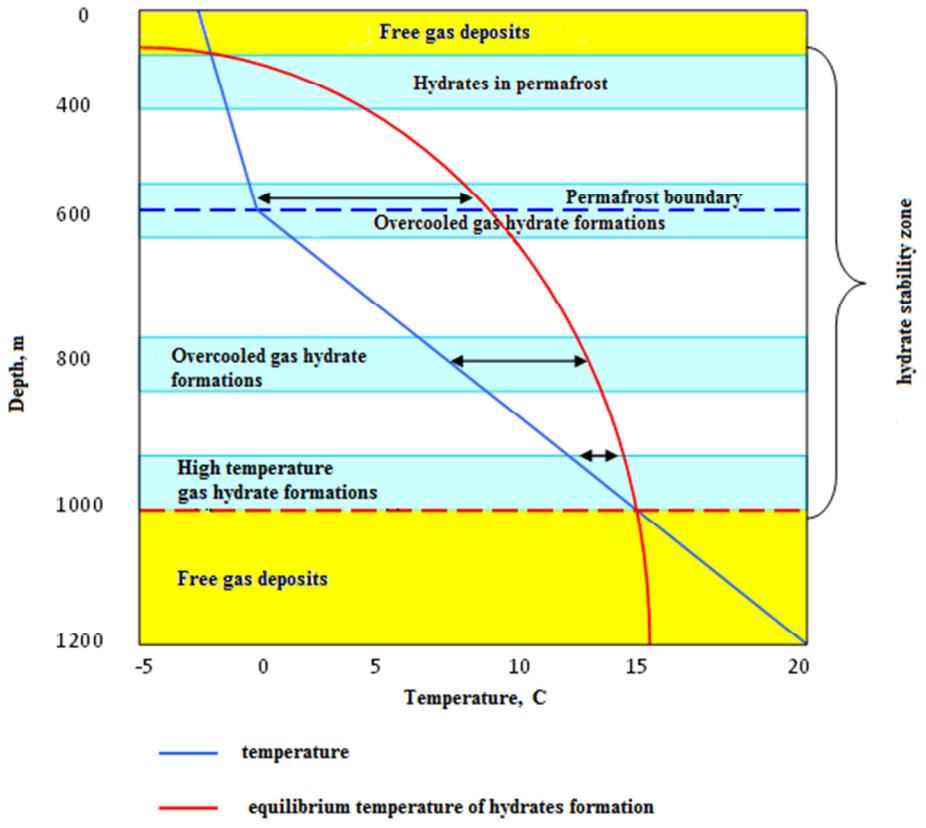

Figure 8 - Classification of gas hydrate reservoirs based on the degree of cooling (Makogon 1965)

Hydrates are usually a part of a load-bearing granular frame. High-drawdown pressure can be a limiting factor in the case of a high degree of overcooling, leading to the destruction of hydrate pore space and sand accumulations at the bottom of the wellbore, in addition to wellbore instability.

Thermal or thermochemical stimulation can be effective in overcooled gas hydrate reservoirs with a high net pay, reducing required pressure drawdown. In the case of significant overcooling (15 to 20K), production from these types of the reservoirs can be unprofitable. This type of hydrate deposit requires a large amount of energy, not

only for hydrate decomposition but also for heating the rocks and fluids around the deposits., Low efficiency of thermal stimulation is due to larger heat loses to the surroundings. All of these conditions are made even more complex by the fact that the rocks with hydrate saturation greater than 35% are virtually impermeable to gas and water due to the low relative permeability to these fluids.

Depressurization is practically unacceptable for offshore gas hydrate deposits where hydrate is the grain's cement. Gas hydrate decomposition will decrease the wellbore stability, which can lead to the destruction of the well and the production platform (Rutqvist J. 2009).

Large-scale international efforts are being made to develop economical technologies for the production of gas from gas hydrates. It is obvious that the development of gas hydrate deposits will require new solutions, new technologies, and newer ways of thinking. Therefore, the commercial development of gas hydrate deposits will begin initially in highly industrialized countries.

In 2002, a thermal method for gas hydrate decomposition was carried out in the Mallik field (Canada) by JOGMEC and Natural Resources Canada (NRCan) (Kurihara et al. 2010). The process involved circulating hot water in the wellbore to increase the temperature and the drawdown pressure; thereby, inducing hydrate decomposition and gas flow to the surface. As a result, the well produced 468 m^3 (16.5 MSCF) of gas during the test (represented by line 3 in Fig.7).

During 2006 and 2007, depressurization methods were used in various hydrate production tests conducted in the Mallik field, resulting in the production of 830 m^3 (29.2 MSCF) of gas and 20 m^3 (170 STB) of water (Kurihara et al. 2010). In 2008, a

long-term production test was conducted for six days and an increase in the production rate was observed compared with the first test; i.e., 13000 m^3 (458 MSCF) of gas and 70 m^3 of water (597 STB) were produced (Kurihara et al. 2010).

In 2012, ConocoPhillips, in partnership with (JOGMEC, conducted a field trial of methane hydrate production by means of chemical injection in Anchorage, Alaska (Schoderbek 2011). This process involved CO_2 injection to induce an in-situ exchange of CO_2 for the methane (CH_4) molecules within a hydrate structure in attempting to release methane for production. As a result of this test, approximately 30000 m^3 (1 MMSCF) of gas was produced over a 40-day test (Schoderbek 2012).

One of the first discoveries of natural gas hydrates was in the Messoyakha field located in northeastern Siberia (Makogon 1984), and this field is currently the only successful example of commercial methane production from gas hydrates. Therefore, an intricate analysis of production operations and reservoir development of this field is imperative and will provide insight into newer solutions and technologies that can possibly be used to address the challenge of gas hydrate production in other regions.

A comparison of the geology of the Messoyakha and Prudhoe Bay-Kuparuk River hydrate accumulations suggests that the Alaskan gas hydrates may also be a producible source of natural gas (Krason 2000). The gas hydrate potential of the Prudhoe Bay-Kuparuk River region is estimated to contain approximately 1.0 to 1.2 trillion cubic meters of gas (35 to 42 TSCF), which is 15 times greater than gas resources in the Messoyakha field. This indicates that the gas hydrates of northern Alaska may be an important source of natural gas in the near future (Collett 1992). Production and completion techniques can be similar to the ones applied in the Messoyakha field. A

production history and productivity analysis of the Messoyakha field can provide highly valuable information that might lead to newer solutions and technologies and pave the way for newer ways to develop gas hydrate reservoirs worldwide.

1.5. Literature review and scope of the study

The successful development of the Messoyakha field attracted tremendous attention to the potential for gas hydrates as a future gas resource. The oil and gas industry has shown enormous interest in analyzing the reservoir behavior of the Messoyakha field. More than 100 papers have been published by several authors to prove or disprove the presence of hydrate in the Messoyakha (Bogatirenko 1977). A number of papers have also been published to analyze the pressure and temperature regimes and also to re-examine the geological and geophysical parameters of this reservoir (Schoderbek 2011).

Initially, the Messoyakha field was described as a water-drive gas reservoir. After the discovery of naturally occurring gas hydrates (Makogon 1966), the field has since been described as a gas reservoir overlaid by gas hydrates and under laid by an aquifer (Krason 2000). However, there is no current scientific consensus on the reservoir description (Collett and Ginsburg 1997). It has also been observed by many researchers that unconventional phenomena have occurred in the Messoyakha field during its production. This phenomena has indicated the possible presence of gas hydrates (Makogon 1981) and may lead to a more complete description of the reservoir. Analysis of these data is vital to explaining the observed phenomena and characterizing the reservoir.

The evidence for gas hydrates in the Messoyakha field was re-examined and the available geologic data were critically reviewed to determine if gas hydrates contributed to gas production (Collett and Ginsburg 1997). These authors concluded that hydrates may not have contributed to the gas production at Messoyakha field. Moreover, they provided a viable non-hydrate hypothesis, showing that the production history could be misleading and cannot be used as a conclusive evidence to prove the presence of gas hydrates. This viewpoint will be examined in our work by the field test results conducted in the several wells.

Collett suggested that the Prudhoe Bay-Kuparuk River field and the Messoyakha field have similar geological parameters. He also suggested that the gas-hydrate-depressurization production scheme used in the Messoyakha field might have a direct application in the hydrates in northern Alaska (Collett 1992). Therefore, the analysis of the production operations in the Messoyakha field can be instrumental in developing and extracting gas from hydrates in the Prudhoe Bay-Kuparuk River field.

A TOUGH simulator was used to analyze the reservoir performance of the Messoyakha field gas hydrate reservoir and to create several 2D cross-sectional models representing the Messoyakha field (Grover et al. 2008). Various reservoir parameters have been studied to determine their influence on gas recovery from hydrate cap reservoirs. Various favorable and detrimental scenarios for producing gas from hydrate reservoirs were described. Based on the 2D reservoir models, it was concluded by Grover that the free-gas hydrate layer is under laid by a free-gas layer with a weak aquifer in the Messoyakha field. In Grover's study, the effect of the aquifer was only investigated for an individual well and no comparison was made with actual field data.

Therefore, we are going to study different aquifer models on a field scale and assess the contribution of the aquifer as a pressure-support mechanism for the reservoir. The VRR (volume replenishment ratio) for early years of production was found to be 15 to 20% for the Messoyakha field. The VRR, over the life of the field, has never been studied in the past, so in the present study, we plan to obtain field-wide VRRs for isothermal and non-isothermal models for the life of the field, which can be useful in forecasting gas hydrate reservoir performance.

Current reserves and OGIP estimations for the Messoyakha field are not accurate. Numbers obtained by project design engineers were validated using different methods (Schoderbek 2011). The difference in OGIP calculations using various methods ranges from 21% to 120% of initial estimation. This wide variation warrants the need for more accurate estimates; therefore, using full-scale model results, we plan to narrow the range of estimated OGIP. Filatov et al. (2008) also admitted that their model does not reflect the true behavior of the aquifer (Filatov 2008). The authors did not study the effect of temperature changes in the field. Therefore, we plan to create a comprehensive model that addresses all of the deficiencies in previous Messoyakha field studies and present a model that is an exact representation of the physics and OGIP estimates of the field.

CHAPTER II

MESSOYAKHA RESERVOIR FEATURES

2.1. Geology of the Messoyakha gas hydrate reservoir

The Messoyakha field is the most famous example of a large hydrate accumulation. This reservoir was discovered in 1967, and gas production began in 1969. The initial gas in place by first project estimates, without taking into account the presence of hydrates, was 24 x 10^9 m^3 (847 BSCF).

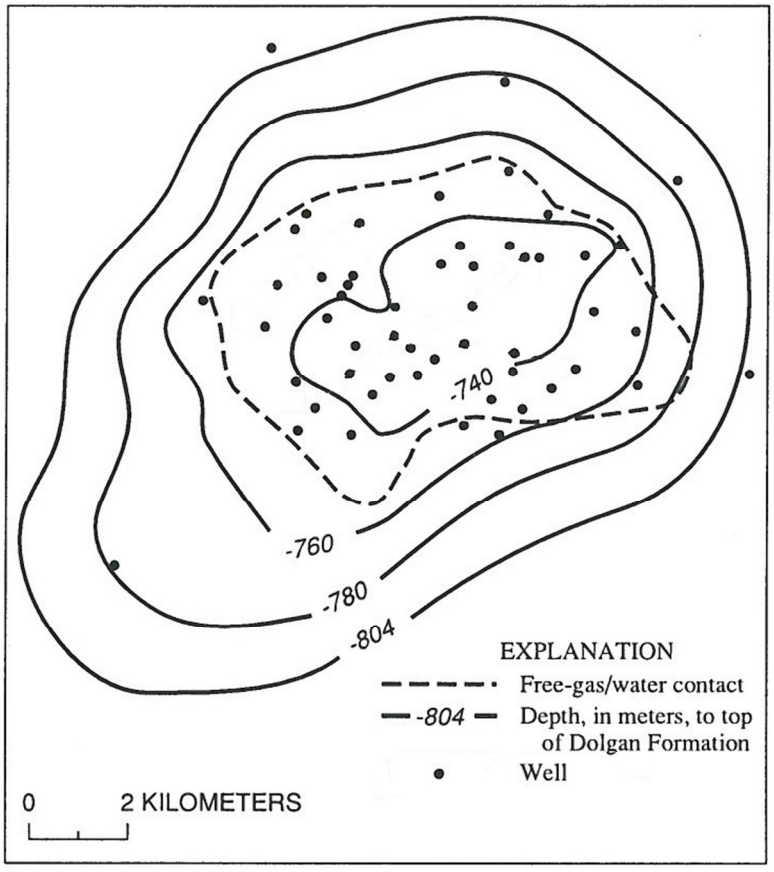

Figure 9 - Structural map of the Messoyakha field (Collett 1992)

The trap type is a Dolgan formation dome of the Albanian-Cenomanian age (Fig. 9). The areal size of the structure is roughly 19 x 10.5 km^2 (11.8 x 6.51 miles) (Filatov 2008), and he structure strikes northeast to southwest. The gas/water contact (GWC) is determined to be at – 805 m TVD (– 2,630 ft), and it is not horizontal. The structural map of reservoir top is presented in Fig. 9. The Dolgan formation thickness is 74 m (275.5 ft) with porosity varying from 16% to 38% and a mean value of 25%. Water saturation varies from 29 to 50% with a mean value of 40%. Permeability ranges from several mD to 1 D, with a mean permeability of 203 mD. The initial reservoir pressure was determined to be 7.7 MPa (1,147 psi). The initial composition of the free gas was C_1-98.6%, C_2-0.1%, C_3 -0.1%, CO_2-0.5%, N_2 – 0.7%. Formation water salinity does not exceed 1.5 %. The total OGIP is uncertain due to conflicting hydrate estimates.

Four models of the Messoyakha field structure have been suggested by different authors (Fig.10). All of these models are based on indirect methods, research, and the results of calculations. There was no direct evidence of gas hydrate cap or oil rim in the formation; however, a number of observations show the validity of this models.

The first model was proposed by Makogon. Based on laboratory studies, he argued that the top portion of the reservoir was a hydrate layer with free gas and an aquifer underlying it. Medvedskiy suggested the Messoyakha reservoir is a water-drive gas reservoir with a GWC at 805-m (2,640-ft) TVD. Consulting group "Actual Geology" (model III) proposed that there is an oil rim between the free gas and water layer.

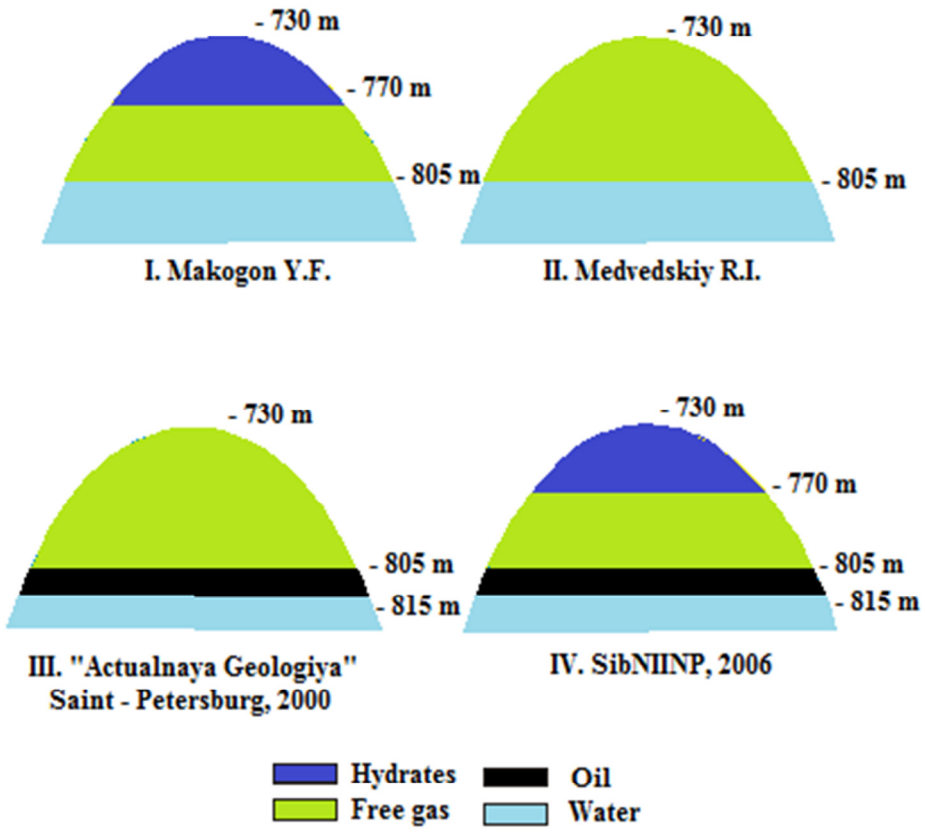

Figure 10 - Models of the Messoyakha reservoir (Filatov 2008)

Their model was based on the observations of residual oil in the cores extracted from several wells in this structure. Finally, a fourth model suggested by Filatov (2008), was based on the existence of the simultaneous presence of an oil rim at the bottom and hydrate cap at the top portion of the Messoyakha anticline trap.

Additional research, direct field tests, and core samples extracted at reservoir temperatures and pressures from hydrate stability zone are required to confirm or refute the validity of any of these models. In the next section, the facts that were used in support of each model will be summarized.

2.2. Attempts to prove the absence of hydrates in the reservoir

A number of investigators have attempted to prove the absence of hydrates in Messoyakha as shown by the consistency of models 2 and 3 (see Fig. 10). Most published studies show that some portion of the Messoyakha lies within the zone of predicted gas-hydrate stability; however, some researchers question the quality of available Messoyakha reservoir temperature and pressure data that are required to assess the potential occurrence of gas hydrates. Ginsburg et al. (1997) argued the opportunity of gas hydrate presence based only on the reservoir temperature and pressure values (t = 8 to 12°C, P = 7.7 MPa or 46 to 54, P= 1128 psi) (Collett and Ginsburg 1997). They suggest that it is impossible to define the conditions of gas hydrate formation existence in the Messoyakha field because of the limited and poor reservoir pressure and temperature data and the highly variable compositions of the sampled reservoir gases and waters (Collett and Ginsburg 1997). However, the absence of data or the quality of data does not disprove the presence of hydrates.

Another argument, based on the assumption that OGIP calculations initially were incorrect, suggested that the pressure-support mechanism could be due to the interflows between the productive layers and hydrates in the porous media. Secondary hydrates could be formed due to the development activity (Collett and Ginsburg 1997) because the temperature drop due to the Joule - Thomson effect leads to the formation of gas hydrates in the wellbore vicinity. The most recent objective studies show that even if there were any hydrates in the Messoyakha field, the gas hydrate saturation would not exceed 5% (Collett and Ginsburg 1997).

Ginsburg (1997) argued that for many years, the production history of the Messoyakha field and results of associated production tests have been used as evidence for the presence of gas hydrates. Ginsburg provided a viable nonhydrate alternative to explain the Messoyakha field production history. The alternative explanation shows that such a pressure support observed in the Messoyakha field could be due to interflows between the upper and lower formations, which can be recognized by means of gas composition changes. He used the composition of CO_2, C_2H_6, C_3H_8, and He as evidence, but the differences in gas compositions are inconclusive because of the measurement quality. The presence of He in the Messoyakha field does not form hydrates, and its content changes in the gas composition are determined by convective diffusion and gravitational redistribution in static and dynamic conditions during shut-in and work periods and cannot be used as a direct proof of gas hydrate absence.

Ginsburg et al. (1997) believed that increases in gas production rates after methanol treatment tests in the Messoyakha field were due to the dissociation of technogenic gas hydrates rather than natural gas hydrates. However, the results obtained by Sapir during methanol injection tests in the Well #156 show that the decomposition area is much larger than the areal formation water intrusion during drilling operations (Bogatirenko 1977).

The volume of water produced from the Messoyakha field suggests that only a limited amount of the produced gas can be attributed to gas hydrate production. Ginsburg showed that if all of the water produced (4 litres of water/m^3 of gas or 0.178 bbl/MSCF) corresponds to gas-hydrate dissociation, it would account for no more than

0.1% of all the gas recovered and that gas hydrates would not have contributed significantly to gas production in the Messoyakha field.

2.3. The presence of an oil rim in the reservoir

The presence of an oil rim is not confirmed by any direct data. Gas composition is too light to indicate the presence of an oil rim at this time. However, several observed phenomena from a number of wells show the presence of oil in the reservoir (Table 2). The most obvious oil signs were observed in Well #118 (Table 2).

Over geological time due to changing climatic conditions, the Messoyakha field changed its phase state. Approximately 2,000 years ago, the thickness of the permafrost in the region was greater than 500 m (1,640 ft) , and the Messoyakha field was a fully hydrate field. Hydrates could be in contact with the oil rim or directly with the aquifer, depending on the specific temperature and pressure conditions. Free gas could not have accumulated due to pressure and temperature conditions. An increase in reservoir temperature during the climatic changes led to hydrate decomposition and formation of a free-gas layer that pushed the oil out of the anticline.

Table 2 - Oil Observations At the Messoyakha Field (Filatov 2008).

Well #	Interval, m	Character of oil features
2	828-835	Sandstone and sand with oil smell
3	826-834	Sandstone of yellow and grey color with gasoline smell
	854-875	Sandstone of yellow and grey color with gasoline smell
7	830-845	Sandstone poorly saturated with oil or oil smell
	868-883	Sandstone with oil smell
9	811-831	Sandstone of yellow and brown color with gasoline smell
109	870-877	Fine-grained oil-saturated sandstone
118	839-865	Sandstone of light brown color with residual oil and oil smell
	869-873	Sandstone of light brown color with residual oil and oil smell
	889-900	Sandstone of light brown color with residual oil and oil smell
145	876-881	Sandstone with remains of bitumen
160	840-876	Sandstone of grey and yellow color with oil smell

During these phase transitions, the GWC contact was migrating in the range of 15 m (50 ft). An oil rim of about 15-m (50-ft) thick could exist at the depth of 790 to 815 m (2,590 to 2,675 ft). Prior to the beginning of field development, all of the oil was pushed out of the formation to the nearest traps. The oil rim is most likely absent at this time (Fig. 11).

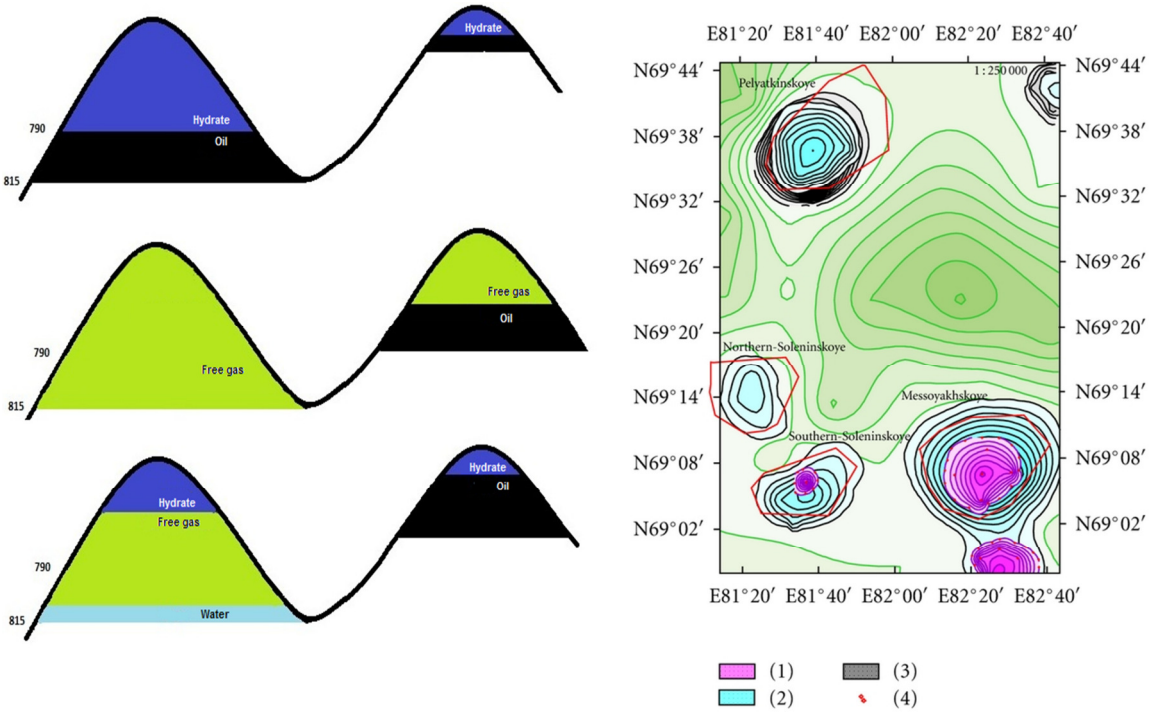

Figure 11 - Oil migration during the climate changes in the Messoyakha gas hydrate field. The map of hydrocarbon accumulation zones produced from satellite data processing results for the Messoyakha gas-hydrate deposit area (western Siberia, Russia). (1) Zone of gas-hydrate deposits; (2) zone of gas deposits; (3) zone of oil deposits; (4) points of the anomalous responses registration from gas-hydrate deposits

More than 170 x 10^6 m^3 (1,491 x 10^6 STB) of oil could have been pushed out from the Messoyakha deposit over the last gas phase change cycle. This oil might be found in nearby traps. At 25% recovery efficiency and a market price of oil of \$400/ m^3 (80 \$/bbl), the potential cost of crude oil will exceed 20 x 10^9 \$/bbl.

2.4. Justification of hydrates presence in the Messoyakha field

The majority of scientists studying hydrates believe that the Messoyakha field contains gas hydrates mainly due to initial reservoir pressure and temperature (P = 7.7MPa, t = 8 to 12°C or P=1128 psi, t=46-54 F) that are within the gas hydrate formation window (Makogon 1984). The analysis of subsurface temperatures, reservoir

pressures, and salinities of pore water suggests that the zone of methane hydrate stability may extend to a TVD of 1000 m (3,280 ft) at the north area of western Siberia. Production has been obtained from a depth interval between 720 m (2,360 ft) and 820 m (2,690 ft). The upper portion of the reservoir, which is approximately 40 m (130 ft) thick, is within the methane hydrate stability zone. If the initial reservoir pressure was 7.7 MPa (1,145 psi), then the equilibrium temperature was 10°C (50°F). This isotherm defines the lower boundary of free-gas and gas hydrate accumulations.

Low gas rates during production tests in the upper portion of the Messoyakha reservoir produced the first physical evidence of possible in-situ gas-hydrate occurrences (Table 3 and 4). Analysis of spontaneous potential and caliper well logs from 57 wells drilled in the Messoyakha field reveal the presence of apparently frozen rock intervals within the Dolgan formation (Makogon 1984), obviously containing in-situ gas hydrates rather than ice at these depths (730–800 m, t = 8–12°C, permafrost depth = 450 m).

Further analysis of electrical resistivity well logs also indicated the presence of gas hydrates in the upper section of the Messoyakha gas accumulation (Makogon 1981). The gas hydrate and free-gas portions of the Messoyakha field are depicted in the generalized cross section shown in the figure on page the #41.

Table 3 - Inflow Performance of The Messoyakha Wells From The Top Section of The Reservoir (Makogon 1981)

Well #	Test interval	Fluid	Production rate		
			gas rate, 10^3 m^3/D		water, m^3/D
	Depth, m		During the test	Open flow potential	Prod rate of water
1	826-837	gas+water	28.3	-	-
5	810-820	water+gas	weak inflow	-	50
6	832-838	gas	3.2	-	-
117	843-851	water	-	-	-
121	815-826	gas+water	15.8	26.2	-
123	830-843 845-854	gas	8.6	-	-

Table 4 - Well Productivity Comparison of Wells Completed in the Free-Gas and Gas Hydrate Zones (Makogon 1981)

Well #	Absolute depth	Abs depth of isotherm 10°C	Distance to the perforations	Open flow potential
121	-716-727	-791	64	26
109	-748-794	-800	6	133
150	-741-793	-787	-6	413
159	-779-795	-766	-29	626
131	-771-793	-734	-59	1000

Measured flow rates from the free-gas section of the reservoir were substantially greater than those from the gas-hydrate section (Table 4). To confirm the presence of gas hydrates within the upper section of the Messoyakha field, a series of hydrate-inhibitor injection tests was conducted. During these tests, substances, such as methanol and

calcium chloride, which destabilize and prevent the formation of gas hydrates were injected into the suspected gas-hydrate-bearing rock units (Table 5).

Table 5 - Productivity Increase After Methanol Treatment in the Well #133 and 142 (Makogon 1981)

	Before treatment		After treatment	
#	Draw-down pressure, atm	Production rate, 10^3 m^3/D	Draw-down pressure, atm	Production rate, 10^3 m^3/D
133	3.5	25	0.4	50
	7	50	0.8	100
	14	100	1.1	150
	19	150	1.5	200
	22	200	2	250
142	8	5	0.4	50
	13	10	0.5	100
	19.5	25	0.7	150
	25	50	1	200
	30	100	1.4	300
	33	150		

Most of these tests summarized by Makogon (Makogon 1981) resulted in dramatic increases in production rates that were attributed to the dissociation of in-situ gas hydrates. Long-term production from the gas-hydrate section of the Messoyakha field has been achieved by a simple depressurization scheme. The behavior of reservoir pressure can be considered to be further evidence of gas hydrates presence and will be discussed later.

2.5. Justification of hydrate presence and calculation of hydrate saturation in the Messoyakha deposit

A direct method was used to confirm the presence of gas hydrate deposits in the Messoyakha field. Because the productive layer in all of the wells were cased and cemented, excluding any chance of direct core sampling, Ginsburg and Sapir proposed a method of gas hydrate saturation determination based on the thermodynamic effect of the interaction of methanol with the saturating reservoir fluids, gas, water, and gas hydrates. The results of the methanol interaction with these fluids are different. When injecting methanol into the aquifer, the bottom hole temperature increase will be recorded as negative enthalpy from mixing water and methanol. Cooling of the wellbore and wellbore vicinity occurs during methanol injections in a gas-hydrate formation because the enthalpy of hydrate decomposition and evaporation of water in the gas phase are positive. However, the thermal effect of methanol evaporation is much lower than the cooling effect of the decomposition of hydrates because the evaporation in the reservoir conditions is low. The total heat of the dissolution and evaporation processes $dH_{ev} + dH_{dis} = -9.19 + 3.89 = -5.8$ kcal / mol (23.4 Btu/mol) is three to five times lower than the enthalpy of dissociation of gas hydrates (14 to 32 kcal / mol (55 to 125 Btu/mol)).

Well #156 was chosen for the experiment of methanol injection because it penetrated only the top two suspected hydrate saturated formations in the MD range 819–828 and 830–836 m (2,686–2,715 and 2,722–2742 ft) (Bogatirenko 1977). Hydrate saturation is estimated to be 70 to 80% in the upper layer and 30 to 40% in the lower layer. Commercial flow rate was not achieved from this well initially.

Repeated methanol bottomhole treatment did not lead to a positive effect, indicating a low-permeability reservoir, which did not allow of formation of hydrates during drilling. Methanol did not penetrate into the formation easily; thus, ensuring maximum contact with the hydrate over the entire zone of the perforation interval.

A quantity of 4 m^3 (34 STB) of methanol (concentration 96%) was pumped into the well with 1 m^3 (8.52 STB) into the tubing and 3 m^3 (25.5 STB) in the annulus, which equalized the fluid levels. The temperature of injected methanol was 4°C (40°F). The main phase of the experiment, which extended over four days, was to conduct periodic downhole measurements of temperature and continuous recording of pressure at the wellhead. The results obtained in the experiment are summarized in Table 6.

The temperature behavior in the borehole allows for subdividing the entire experiment into four stages where the main role of the temperature field belongs to the various reactions occurring in the borehole. The first measurement (0 step) when the methanol is injected into the well, describes the temperature distribution along the wellbore, which is close to the natural temperature field of the surrounding rocks. The second stage (1–3 measurements), after the injection of methanol, corresponds to the period of predominance of the thermal effect of the exothermic reaction of mixing methanol and water in the bottom hole (in the depth interval 834–897 m (2,735–2,942 ft)). The result is a rapid recovery of the temperature field, impaired by pumping a large volume of cold methanol into the well.

The third stage (4–8 measurements) is characterized by a progressive decrease in temperature around the wellbore caused by the endothermic reaction constantly taking place in the bottom hole.

The fourth stage (nine measurements) shows the intensity decrease of the endothermic reaction of hydrate decomposition, and the beginning of the restoration of the natural temperature field. The time of full restoration of the initial bottom-hole temperature was not achieved, and the experiment was terminated. The temperature gradient along the wellbore during the third stage indicates that the intensity of heat transfer between fluid in the well and the formation up the wellbore decreases. This phenomenon suggests that the heat balance of the well is provided by the flow of gas passing through the wellbore. The progressive cooling of the wellbore could only be caused by a constant reaction from decomposition of hydrates. If the productive layer did not contain hydrates, the temperature of the gas entering the wellbore would be dependent only on the Joule - Thomson coefficient. In this case, a slightly higher temperature would be expected after the injection of methanol than the temperature of the 0 step measurement in which the magnitude of drawdown exceeds that for all subsequent measurements.

These experimental results indicate the presence of gas hydrates in the reservoir. The statement that hydrates are in the reservoir, not at the bottom of the hole and in the perforations, is based on the repeated methanol treatments of the wellbore prior to the experiment.

Table 6 - The Results of The Experiments of Methanol Injections at Messoyakha Field (Bogatirenko 1977).

# of test	Date and Time	Duration, min	T perforations	Pressure, atm				Level of liquid, m
				Dynamic		Static		
				tub	an	tub	an	
0	27/6 - 3 pm	45	9.7	-	-	69	68	834
Methanol injection	28/VI - 5-30 pm	-	-	-	-	56	56	466
1	28/VI - 6-30 pm	45	9.2	34	-	49	-	-
2	28/VI - 9-25 pm	30	9.7	-	-	-	-	-
3	29/VI - 11-10 am	40	9.8	-	-	-	-	500
4	29/VI - 7-50 pm	40	9.1	-	-	-	-	-
5	29/VI - 8-40 pm	40	8.7	-	-	-	-	-
6	30/VI - 11-00 am	40	8.1	31	49	61	65	-
7	30/VI - 12-00 am	40	8	31	49	61	65	-
8	1/VII 1-45 am	40	7.8	-	-	-	-	-
9	1/VII 3-45 pm	40	8.2	-	-	-	-	-

The decomposed hydrates were natural, not induced by drilling, which was confirmed by comparing the volume of hydrate decomposed during the experiment with the volume that could be formed during the drilling operations. The volume of hydrate decomposed was determined by quantifying the total heat of the endothermic reaction at the 3rd stage of the experiment.

Using the Fourier heat conduction partial differential equation of second order allowed for deriving the temperature distribution equation for this experiment.

$$T(R-r,h,t) =$$

$$= \mathrm{Tp} + \frac{\left(\frac{q_1 m_1 \beta_1}{V_1 C_P \rho_P} + \frac{q_2 m_2}{V_2 C_P \rho_P}\right) + \frac{\pi R^2 \Delta T_{sk}}{8 a_{gr} t_1} \exp\left(-\frac{R^2}{4 a_{gr} t}\right)}{1 + \frac{R\alpha}{2\alpha_{gr} a_p t} \exp\left(-\frac{R^2}{4 a_{gr} t}\right)} \exp\left(-\frac{(R-r)^2}{4 a_p t}\right) \qquad (1)$$

$$- \left(\frac{q_1 m_1 \beta_1}{V_1 C_P \rho_P} + \frac{q_2 m_2}{V_2 C_P \rho_P}\right) t_1$$

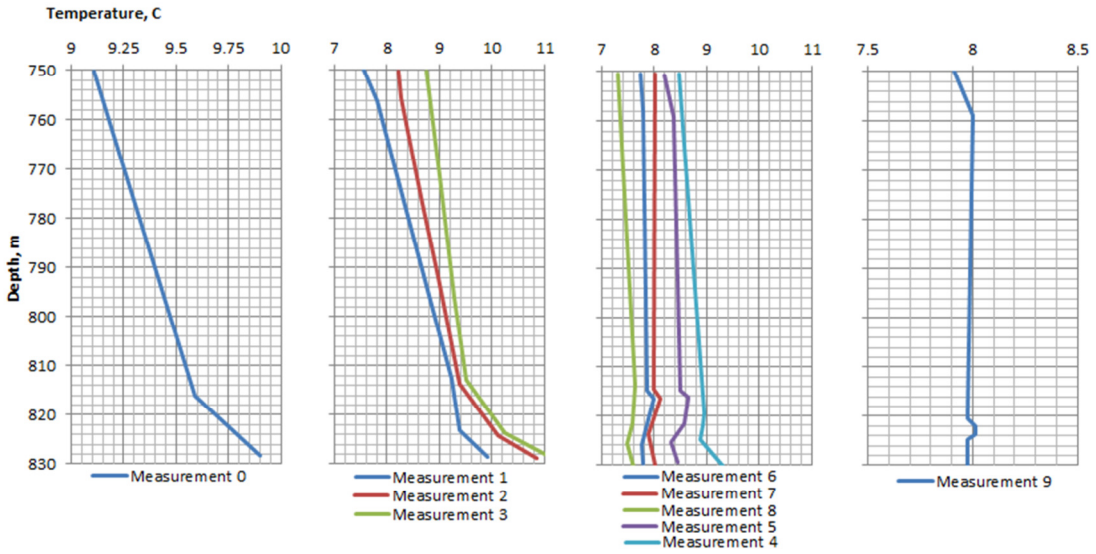

Figure 12 - The field temperature change in the well during the experiment (Bogatirenko 1977).

The dynamics of the temperature field in the borehole is shown in Fig.12. During the 3rd step of the experiment, the volume of the evolved gas was 175 000 m^3 (6.175 MMSCF); hence, the volume of the decomposed hydrate was approximately 1000 m^3 (35 MSCF). The radius of the reservoir where hydrate was decomposed under the influence of methanol was determined to be 142 cm (4.65 ft). We used the following initial data in our calculations: 12-m (40-ft) effective reservoir thickness, 30% porosity,

and 0.5 hydrate saturation. The maximum radius of mud infiltration was estimated to be 0.39 m (1.25 ft) at the wells that penetrated free-gas formations.

A comparison of these two radii (1.49 and 0.39 m) indicates that one methanol treatment took two days to respond fully, leading to the decomposition of hydrates at the bottom hole and at a distance much greater than the distance where hydrates could be formed in the wellbore vicinity while drilling. Hence, the results of the experiment indicate the presence of natural hydrates in the reservoir.

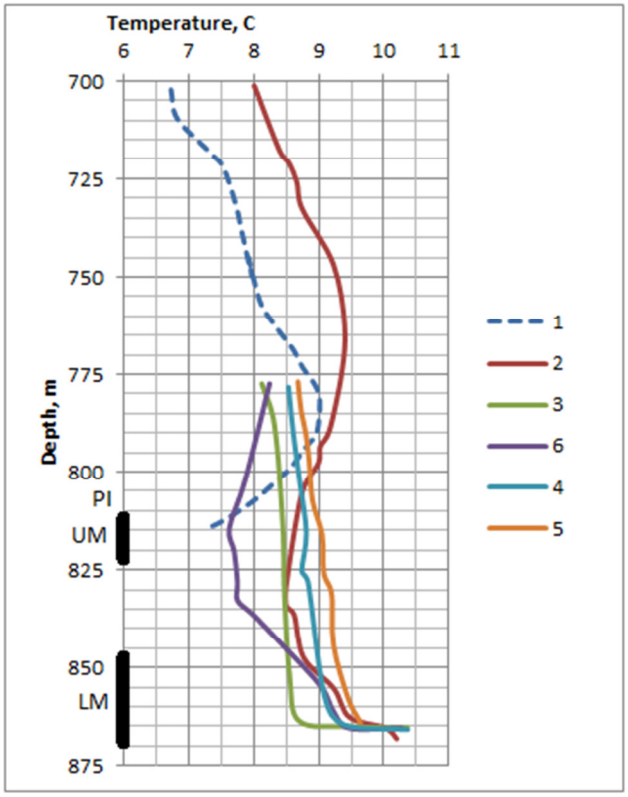

Figure 13 - Temperature well logs (1976, 1985) from Well #142 in the Messoyakha field where 1, 2, 6 = shut-in test, and 3, 4, 5 = during production (Collett and Ginsburg 1997).

Temperature logs confirm gas hydrate presence in the formation even though they are used by some authors (Collett and Ginsburg 1997) as evidence of gas hydrate

absence. As shown in Fig. 13, the temperature during shut-in periods is lower in the hydrate saturated intervals because endothermic reaction of hydrate decomposition was occurring in these intervals. As soon as the well was shut in, the temperature field restoration began; thus, during production periods, the argument that temperature should be the lowest is a misunderstanding of the measuring process. The temperature measuring device is located in the wellbore and does not measure the temperature of the layer but rather it only measures the temperature of the flow that consists of the mixture of warm gas from lower free-gas layer and cold gas from the decomposition area. Because the hydrate saturated layers are less productive, their contribution to the temperature of the gas mixture in the well in dynamic conditions appears to be higher than the original temperature distribution in the formation. The measurements in static conditions clearly indicate the decomposition of hydrates (Fig. 13).

2.6. Hydrate model of the Messoyakha field

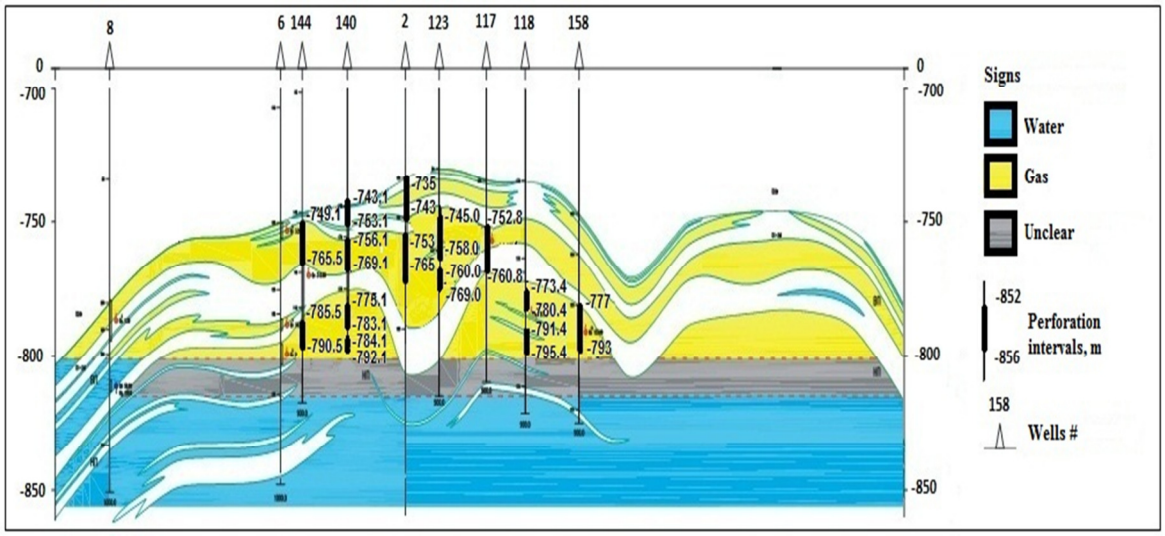

Figure 14 - The cross section of the Messoyakha gas hydrate reservoir (Filatov 2008)

Currently, there is no consensus among scientists about the hydrate presence in the Messoyakha field. Apparently, the only way to confirm or refute this question is by drilling a well with proper coring sampling and testing. In this study, we will rely on the model proposed by Dr. Makogon (1970) and attempt to prove hydrate presence.

According to Dr. Makogon's model, the gas hydrate–free-gas contact is determined to be at a depth of –770 m (–2,526 ft) in the central portion of the field (Fig.14). This section of the field is most likely angulated due to the fact that the isotherms are parallel to stratigraphic lines. The productivities of different intervals also indicate that the free-gas–gas hydrate interface is not horizontal (Fig. 15). The boundary of phase transition interface is at the level where reservoir temperature is near 10°C (50°F). The thermodynamic interface between the gas hydrate and free-gas layers do not have a lithological interface. The hydrate-saturated intervals are located in the layers where the thermodynamic equilibrium exists, and free gas is present below the equilibrium curve.

Productive layers are divided into two deposits: (1) free gas that is located below the equilibrium surface; and (2) gas hydrate, which is located above the equilibrium surface (Fig. 16). The GTG (geothermal gradient) in the interval of the permafrost layers (up to 475 m) is on the order of 1 C/100 m (0.1 F/ft). The GTG under the permafrost layers is 3.0°C/100 m (0.114 F/ft). The temperature at the top of the deposit is 8°C (46 F); whereas at the bottom, it is 12°C (54 F). The GTG in the productive portion of the deposit is 4.2°C/100 m (0.12 F/ft).

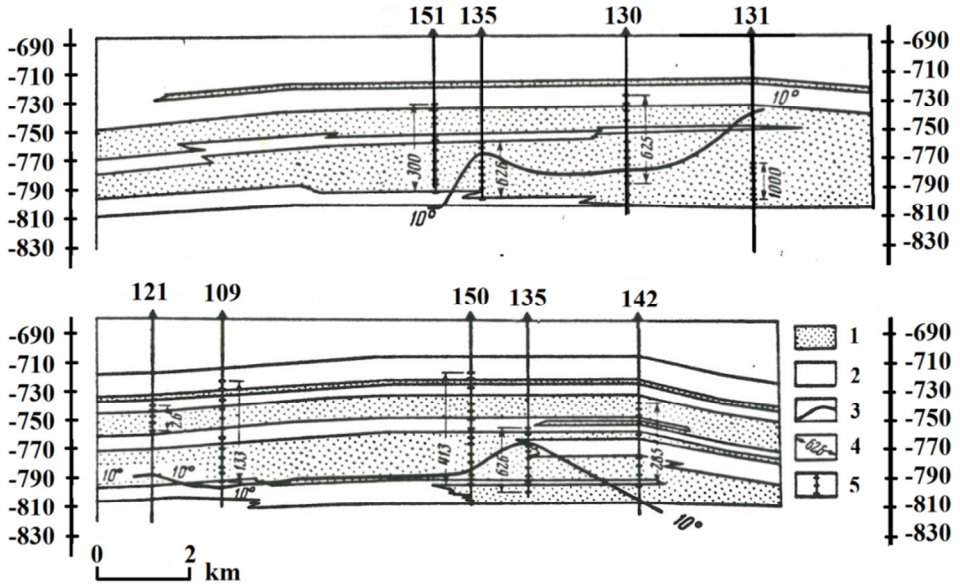

Figure 15 - Temperature profile in the Messoyakha field

Hydrate saturation of pore space in the initial stage of development was unknown. The maximum degree of overcooling in the reservoir prior to the beginning of development did not exceed 2°C (4 F) (at the top of the upper productive layer). The average overcooling temperature was 1°C (2 F). Low overcooling allowed the decomposition of hydrates even with an insignificant decrease in the reservoir pressure.

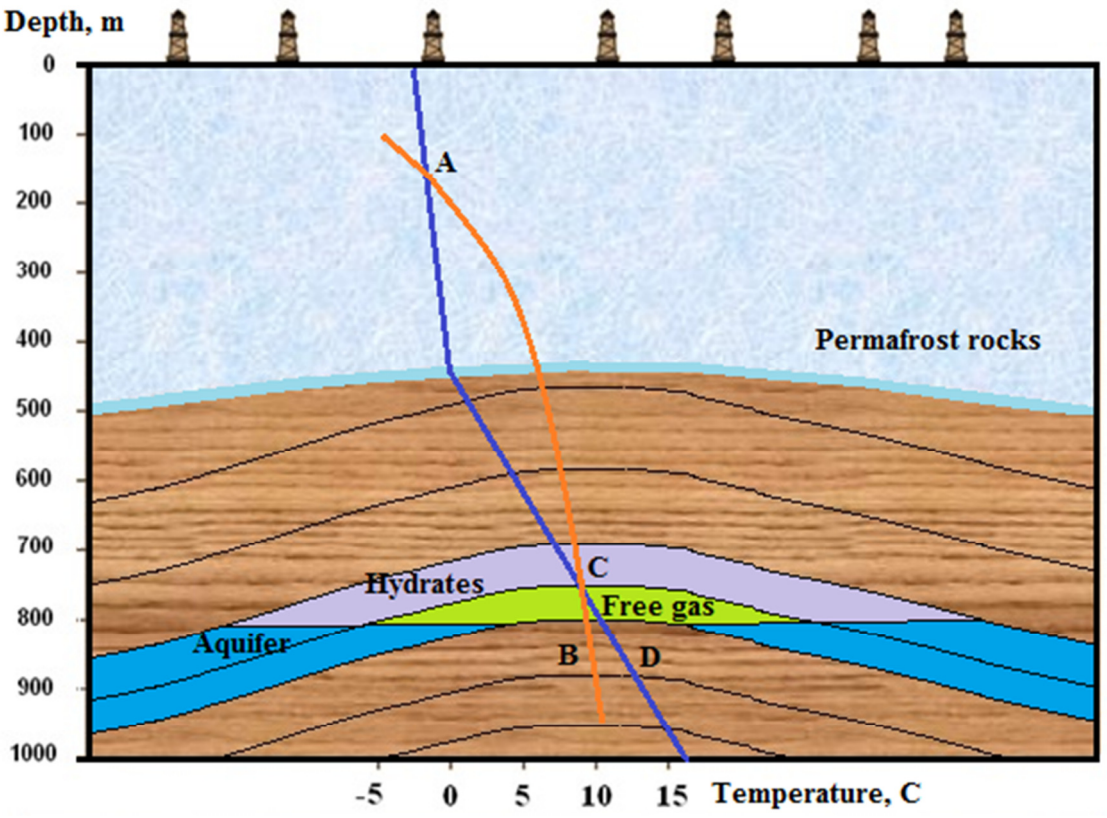

Figure 16 - Temperature profile of the Messoyakha field. Line AB= hydrate equilibrium temperature; line AD = temperature distribution in the cross section

2.7. Production history

Conventional oil and gas production methods have been used to develop the Messoyakha gas hydrate deposit. To date, 61 wells have been drilled within the Messoyakha structure with an average well spacing of 500 to 1000 m (1,640 to 3,280 ft, 40 and 80 acres). Gas production commenced in 1970 and continued until 1977 at an average of 3 x 10^6 m^3/D (115 MMSCF/D). Following a four-year shut-in period, production was reestablished at rates of 0.2 to 0.5 x 10^6 m^3/D (7 to 18 MMSCF/D). Fig.17 shows the gas production and the actual and calculated reservoir pressure during the production and shut-in periods.

The Messoyakha deposit development can be divided into five distinct periods (Fig. 17). The reservoir pressure after 35 years of development decreased from 7.7 MPa (1,128 psi) to 6.0 MPa (882 psi). In the absence of hydrate, the reservoir pressure should be 36 bar (529 psi). With high rates of gas production, the reservoir pressure decreased to 50 bar (735 psi), which was less than the equilibrium pressure by 1.6 MPa (235 psi) during the first period (1969–1971). The field-pressure behavior was exactly the same as if the reservoir were a volumetric gas reservoir; however, the active process of hydrate decomposition began, and continued for many years after the pressure dropped below the initial equilibrium pressure at approximately 6 MPa (880 psi). The reservoir pressure during this period of time (1971 –1975) exceeded the theoretically projected value.

The third period (1976–1977) was characterized by the volume of produced gas being equal to the volume of gas obtained from the hydrate decomposition because the reservoir pressure remained almost constant. The field was shut-in from 1978 to 1981. Because the reservoir pressure prior to the shut-in period was below the equilibrium pressure, the process of intensive gas hydrates dissociation continued during that time. The reservoir pressure increased to 6.0 MPa (880 psi); i.e., it returned to equilibrium pressure (Fig. 17).

Since 1982, gas extraction from the reservoir has not exceeded 400 x 10^6 m^3 /year (14.1 BSCF/year), and the reservoir pressure remained relatively constant (approximately 5.8 to 6 MPa). The gas volume produced from the reservoir approximately corresponded to the volume of hydrate gas entering due to dissociation of

hydrates; however, such pressure support could be due to active aquifer behavior. This option will be examined later in the work being reported here.

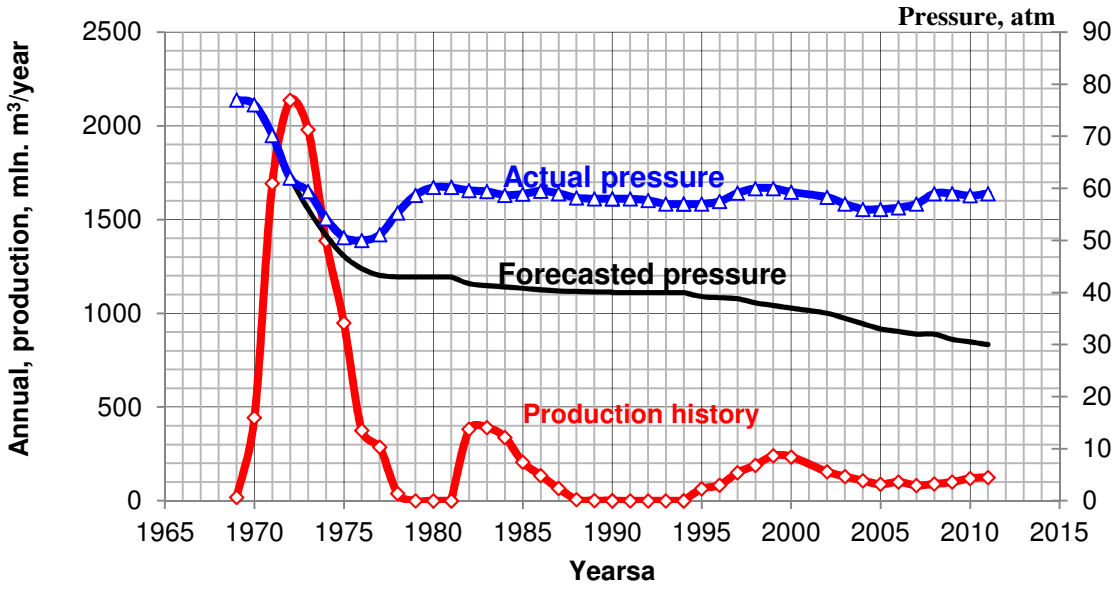

Figure 17 - Reservoir pressure response due to production from the Messoyakha reservoir (Makogon 1981)

The total gas produced from the Messoyakha field as of 1 January 2012 is 12.9 $x10^9$ m^3 (455 BSCF); however, there are no data available on how much gas was obtained due to hydrate decomposition. The average reservoir pressure for 30 years of development has decreased from 7.8 to 6.0 MPa (1146 to 882 psi). According to the field development project, reservoir pressure should be 3.6 MPa (530 psi) in the absence of hydrates.

To answer the question of how much hydrate remains in the reservoir, an exact value of the gas volume initially in place is needed. We examine the numbers obtained by different methods in the following section.

2.8. OGIP in the Messoyakha field

Original gas in place (OGIP) at Messoyakha field was set at 24 billion standard m^3 (846 BSCF). This value was obtained by the project engineers, assuming that the Messoyakha field was a volumetric gas reservoir (Makogon 1981). Based on the data from 61 wells, we attempted to verify this number using different techniques as well as performing some sensitivity analysis.

The volume of gas in the reservoir can be calculated using equation (2):

$$OGIP = Ah\phi(1 - S_w)/B_g, \quad (2)$$

The bulk volume was calculated using the trapezoidal rule and is 1.69 x 10^9 m^3. The average porosity is 25.5%, and the average connate water saturation is 40%. Volumetric calculations show that the OGIP in the Messoyakha gas field is 24.08 x 10^9 m^3 (849.7 BSCF), assuming a volumetric gas reservoir, which is almost equal to the value obtained by the project development engineers. However, we did not take into account the presence of gas hydrates. The presence of gas hydrate will boost the OGIP. Because no field tests were run that provide proof of gas hydrate presence at the field, there is a certain uncertainty in the properties of gas hydrate-bearing layers as well as their presence, which requires additional sensitivity analysis and probabilistic calculations to confirm or disprove.

One of the conventional techniques used for volumetric gas reservoirs is the application of p/z plots to define the OGIP. The equation that is used by most reservoir engineers is as follows:

$$\frac{p}{z} = \left(\frac{p}{z}\right)_i - \left(\frac{p}{z}\right)_i \frac{G_p}{G}, \quad (3)$$

With the high rates of gas production, the reservoir pressure was decreased to 5.0 MPa (735 psi), which was less than the equilibrium pressure by 1.6 MPa (235 psi) during the first period (1969–1971). During that time period, the reservoir behavior was close to the volumetric gas reservoir and the OGIP can be obtained by extrapolating the straight line until it intersects the N_p axis. Such a technique provides a value of 24 $x10^9$ m^3 as shown in Fig. 18. The active process of hydrate decomposition began and continued for many years. Reservoir pressure in the second period exceeds the theoretically projected value and remains constant for more than 30 years. Extrapolating the straight line to the intersection with the G_p axis leads to errors in calculating the OGIP as shown in curve 3 in Fig. 18. The actual OGIP value could be obtained when the average reservoir pressure begins to decrease below the equilibrium. To build a straight line, only points below the equilibrium value should be used in calculating OGIP. An example Curve 2 shows that if there all hydrates were to decompose immediately, the OGIP would be 30 x 10^9 m^3 (1058 SCF).

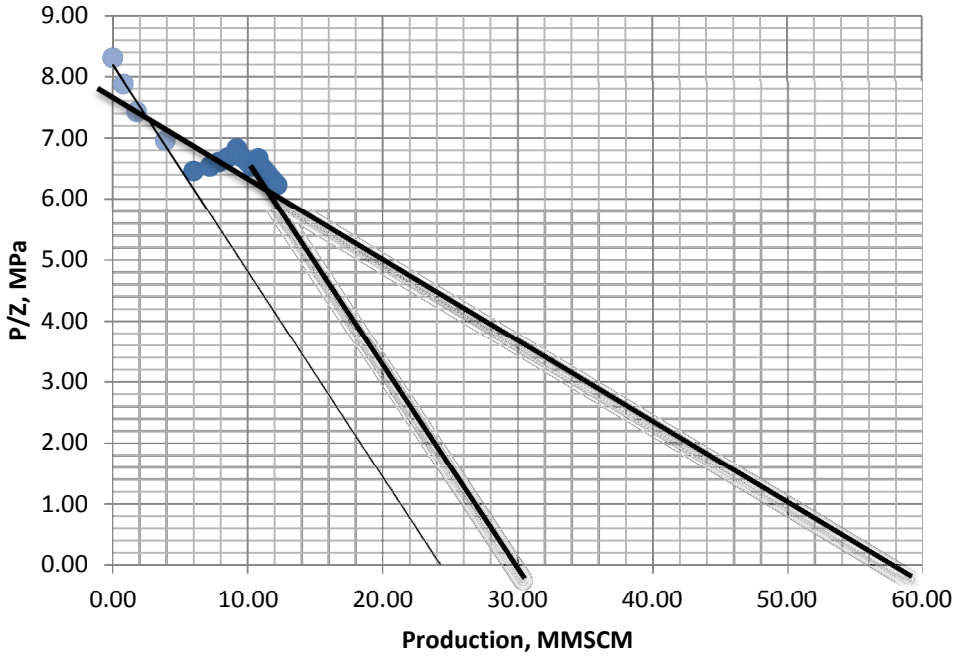

Figure 18 - OGIP in the Messoyakha field using p/z plot

Probabilistic methods were used for OGIP forecasting from the gas hydrate reservoirs with unknown properties. Based on the available well data, we carried out probabilistic OGIP calculations (Table 7).

Table 7 - Comparison of the OGIP Value in the Messoyakha Field Obtained by Different Methods

Comparison of the OGIP value at the Messoyakha field obtained by different methods.	x 10^9 m^3
Geometrical volume of the field	1.62
- free gas part	1.26
- gas hydrate part	0.36
The volume of porous space	0.41
- free gas part	0.32
- gas hydrate part	0.09
Initial gas in place	
- project data	24.00
- volumetric method (no hydrates)	24.1
- p/z plot for the first period (1969-1973)	23.61
- p/z plot for the first period (2006-2012)	18.48
- Monte Carlo simulations (CMOST, @Risk)	
Gas hydrates saturation range 0-20% (@Risk)	23.71
Gas hydrates saturation range 0-40% (@Risk)	27.75
Gas hydrates saturation range 20-40% (@Risk)	31.78
- 3D non isothermal model (CMG STARS)	23.7-36
- 3D isothermal model – pressure support through water and gas injection	31.5

We fitted distributions for the net pays, porosities, and connate water saturations. Drainage areas, based on data from 61 wells, were performed using Monte Carlo simulations using no less than 10,000 iterations. The results obtained are similar to those obtained using the deterministic volumetric method and material balance calculations. Probabilistic methods allowed us to handle uncertainty of gas hydrate saturation as well as the gas hydrate-layer thickness. We performed several case studies for gas hydrate-

saturation distributions. The results obtained from these case studies helped to understand the range of possible OGIP values.

The hydrate layer thickness was fitted to a uniform distribution in the range of 0.3 to 0.7 of the net pay. Assuming no hydrate cap, the expected OGIP value is 23.71 x 10^9 m^3 (836 BSCF). We generated several cases of gas hydrate-saturation distribution to obtain its influence on the final OGIP value. For all cases, hydrate saturation was uniformly distributed within the possible –range. We then generated several cases with the gas hydrate physical distribution over ranges of 0–20, 20–40, and 0–40. The OGIP calculation results can be found in the Table 7.

The OGIP is a function of the reservoir depth, position of the free gas–gas hydrate interface, which is the function of the geothermal gradient, porosity, and gas hydrate saturation. The calculation of the gas in place for any gas hydrate field is a very challenging procedure, which was clearly shown in the Messoyakha gas hydrate field example.

CHAPTER III

COMPUTATIONAL MODEL

3.1. Justification of the model

Application of numerical models allow us to take into account the maximum number of factors that can affect the development of a gas hydrate field, and is the key to solving optimization, control, and field operations management problems. It has been previously shown that the STARS simulator can be used to model hydrate decomposition (Gaddipati 2008).

The STARS simulator is basically designed for non isothermal calculations, and can be used to model hydrate dissociation behavior by making some adjustments to the input parameters. There is a step-by-step procedure for fluid flow simulation problems to obtain final equilibrium conditions for the entire grid as follows:

- Constructing the grid using CMG BUILDER
- Assigning media and rock properties such as permeability, porosity, thermal conductivity, pore-compressibility, and volumetric heat capacity
- Defining components, properties, and all of the reactions and phase transitions between the components
- Specifying rock fluid properties, the capillary pressure model, and initial conditions such as temperature, pressure, water saturation, and mole fraction of components in all phases
- Specifying boundary conditions in the problem by defining wells in the reservoir
- Running the simulation for different time steps specified in the problem

The solution to the problems will be obtained using a 3D orthogonal corner-point grid-block system. The 3D two- and three-phase filtration of gas and water in the pore space is implemented using the hydrodynamic simulator CMG 2010.10.

The initial data for the geological model construction are a set of maps for the reservoir parameter distribution of selected hydrodynamic layers. The maps of the top of the reservoir, porosity, and permeability from the 61 wells were integrated into the grid system. The map of the reservoir top was based on the absolute coordinates data of the top and the bottom of the formations in each well. The surface top was modeled using 50 x 50-m (165 x 165 ft) grid blocks.

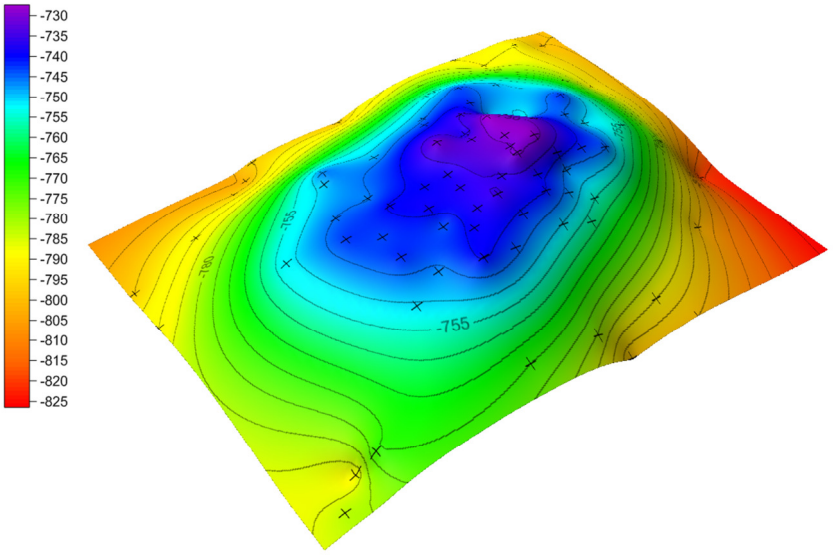

Figure 19 - The top of the DL-1 layer in the Messoyakha field (TVD on the scale)

The total number of active major layers in the hydrodynamic model is 10, and layer thicknesses are in the range of 1–7.4 m (3.28–24 ft). The grid was refined in the central portion of the reservoir to properly reflect the reservoir property changes as well as properly reflect the processes in the central section of the field that has a high

density of the wells. The minimum size of the grid block along the vertical axis is not less than 0.5 m (1.64 ft), which corresponds to a minimum resolution for well logging methods. The major grid block size in the x and y direction is 300 x 300 m (984 x 984 ft). Grid blocks were refined in the central portion of the reservoir with a high-well density. At least a 4 to 5 grid-block spacing was used between neighboring wells in the central area of the field to accurately describe the processes in the area. The size of the grid blocks in the central section of the reservoir range from less than a meter to tens of meters. The underlying aquifer was simulated by the Carter – Tracy infinite extent analytical model.

The distribution of reservoir properties is created within a 3D geological grid. The main assumption made by the method is that it requires the field of 3D distribution of rock types in the space be discrete. This assumption results in making each cell of a 3D grid block system only contain one lithology. The 3D map of the top of the Dolgan formation is presented in Fig.19 and 20.

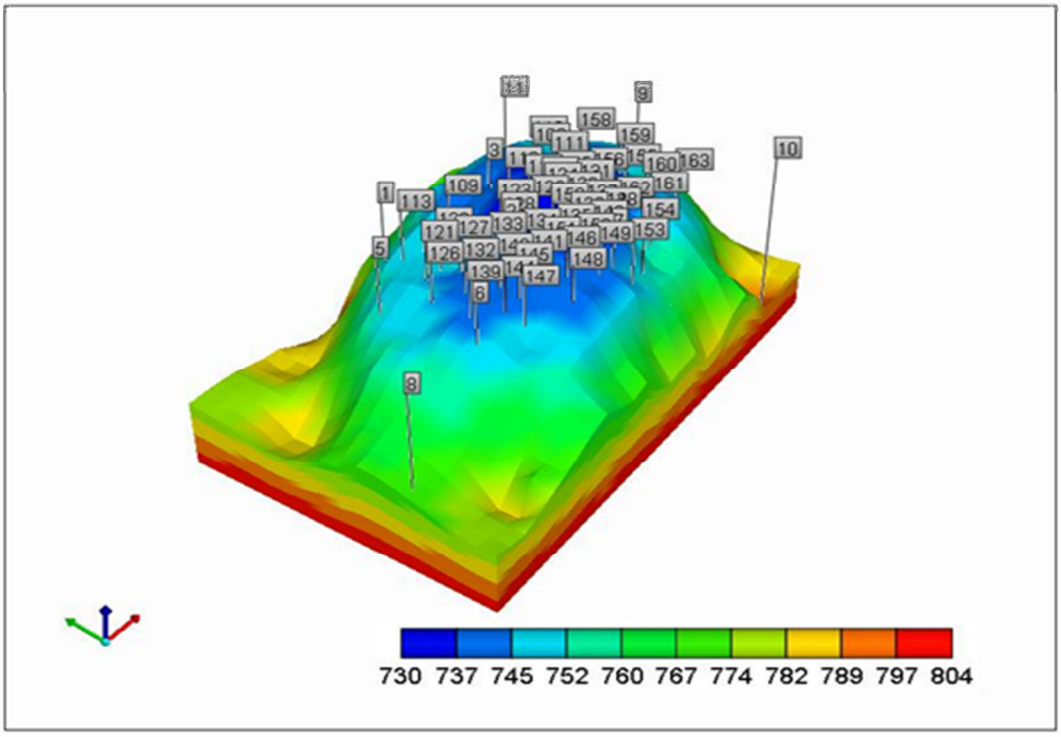

Figure 20 - 3D map of the top of the Dolgan formation (TVD on the scale)

Distribution of porosity and permeability was carried out by an interpolation method using an ordinary Kriging estimation method. This technique provides a smooth change of the parameters in the pinch-areas. Rock compressibility and thermal properties such as heat capacity and thermal conductivity are specified by defining a rock type. Different rock types can be defined within a reservoir.

Capillary pressures are calculated using the Van-Genuchten capillary pressure model. These values are entered in the form of tables in the ROCK FLUID section of the data file. The capillary pressure of water-gas mixture is included as PCOG in the gas-oil table in data file. In the absence of a hydrate phase or oil phase, it is not obvious whether to use capillary pressures as PCOW or PCOG. Using capillary pressure as PCOG gave results that are in agreement with other codes.

Vertical equilibrium calculations of the simulated formation were accomplished using special features of a CMG environment. Gas/water contact was chosen at a TVD of 805 m (2,640 ft). The initial reservoir pressure at a TVD of 780 m (2,558 ft) was chosen as 7.7 MPa (1,146 psi).

The next step in the procedure was to specify different components and their properties. The system defined in this problem is a water-CH_4-hydrate system, which is a three- component, three-phase system. The hydrate can be defined as either an oil phase with very high viscosity or as a solid phase. Each method has advantages and disadvantages. Different components and their physical properties can be directly imported from the simulation software built-in library. An input value of zero for any property returns a standard value already setup in the library of the software package. CMG refers to component molecular weight in kg/gmole. Densities, gas-liquid K values, critical temperature and pressure, and aqueous- and gas-phase viscosities are defined in the following paragraph.

Aqueous and gas mole fractions are calculated based on the pressure and temperature prevailing in a particular cell. Hydrate properties such as molecular weight, critical temperature, and critical pressure are specified in the data file. Due to the wide range of pressure and temperature values in the entire grid, gas/liquid *K* values for water and methane are calculated using the following equation:

$$K = \left(\frac{KV1}{P} + KV2 * P + KV3\right) * EXP\left(\frac{KV4}{T - KV5}\right) \quad (4)$$

The values of KV1, KV2, KV3, KV4, and KV5 for water and methane are pre-defined in the CMG builder.

Gas and liquid heat capacities are a function of temperature and are calculated by the following expressions:

$$CPG = CPG1 + CPG2xT + CPG3xT^2 + CPG4xT^3 \quad (5)$$

$$CPL = CPL1 + CPL2xT + CPL3xT^2 + CPL4xT^3 \quad (6)$$

where *CPG1-4* = the gas heat capcity coefficients, *CPL1-4* = the liquid heat capcity coefficients. The gas component viscosity is given by:

$$visg(i) = avg(i)xT^{bvg(i)} \quad (7)$$

and the liquid component viscosity is given by:

$$viso(i) = avisc(i)\ x\ \exp(\frac{bvisc(i)}{T}) \quad (9)$$

Gas-phase and liquid-phase viscosities are calculated based on the gas- and liquid-component viscosity in the STARS program. The thermal expansion coefficient is expressed as CT1+TxCT2, where CT1 and CT2 are first and second thermal-expansion coefficients.

Hydrate formation and dissociation reactions are specified by equilibrium kinetics. Hydrate dissociation is an endothermic first-order reaction with an enthalpy of -51857 J/gmole and an activation energy of 150218 J/gmole.

$$1\ Hydrate\ \leftrightarrow 6.1\ H_20 + CH_4$$

The equilibrium K value for forward and reverse reactions is given by Eq. (10)

$$K(P,T) = \left(\frac{rxk1}{P} + rxk2\ x\ P + rxk3\right) x\ \exp(\frac{rxk4}{T-rxk5})\ , \quad (10)$$

where rxk1, rxk2, rxk3, rxk4, and rxk5 are correlation coefficients.

After completing all the necessary stages in building the geological model, the geological reserves of the Messoyakha field were calculated under the assumption it was

a volumetric gas reservoir. The total volume of porous space was 1.69×10^9 m^3 (60×10^9 SCF) and the corresponding OGIP value was 24.08×10^9 m^3 (850×10^9 SCF), which corresponds to the value obtained by development engineers.

3.2. Adaptation of the hydrodynamic model for the development history

During the adaptation of the model, the entire production history of the Messoyakha field development as a volumetric gas reservoir was history matched. The goal was to obtain the same pressure history in response to the same production rates as they appeared in practice.

Annual reports and values of reservoir and bottomhole pressures were used as input information. These data have been implemented into the hydrodynamic numerical model as constraining conditions in the wells. Individual well constraints and group-control constraints were used to maintain annual gas production from the field at actual levels. The CMG IMEX black-oil isothermal simulator was used to predict the Messoyakha reservoir behavior as a volumetric gas reservoir. Reservoir properties were calibrated to reflect the actual pressure behavior. Comparison of actual gas production and results obtained by the model are shown in Fig.21.

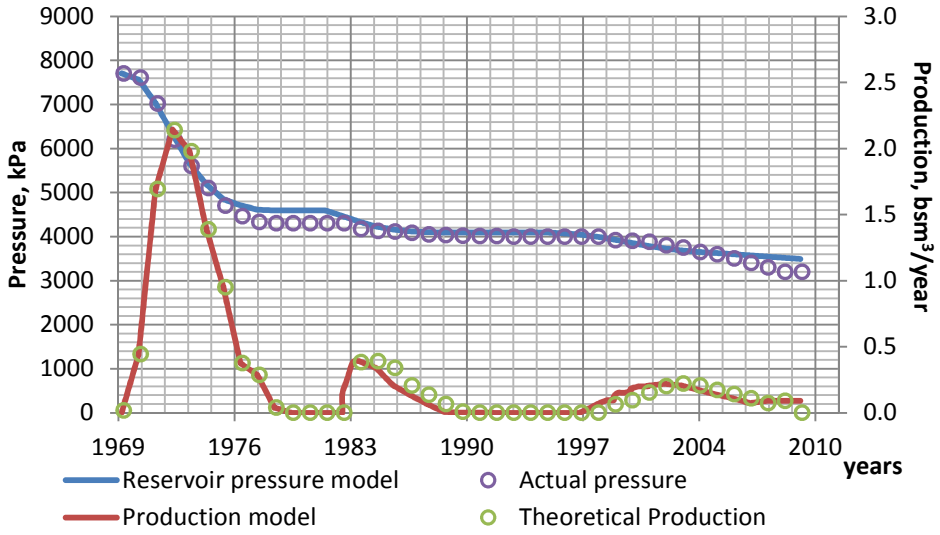

Figure 21 - Actual field data compared with the results obtained by the model

Different aquifer models were investigated to determine if the actual reservoir behavior could be obtained through water encroachment. Specifically, the Carter Tracy infinite-extent analytical model was used to model aquifers of different strengths.

Aquifers with different strengths were studied as alternative pressure support mechanisms. With active aquifer support, the average reservoir pressure decline will be offset by water intrusion. During reservoir production, water will encroach the formation and occupy the pore space that previously contained gas. It is possible that an active aquifer beneath the Messoyakha reservoir exists and could provide the necessary water support to match the actual pressure history obtained. The results of calculation are shown in Fig. 22.

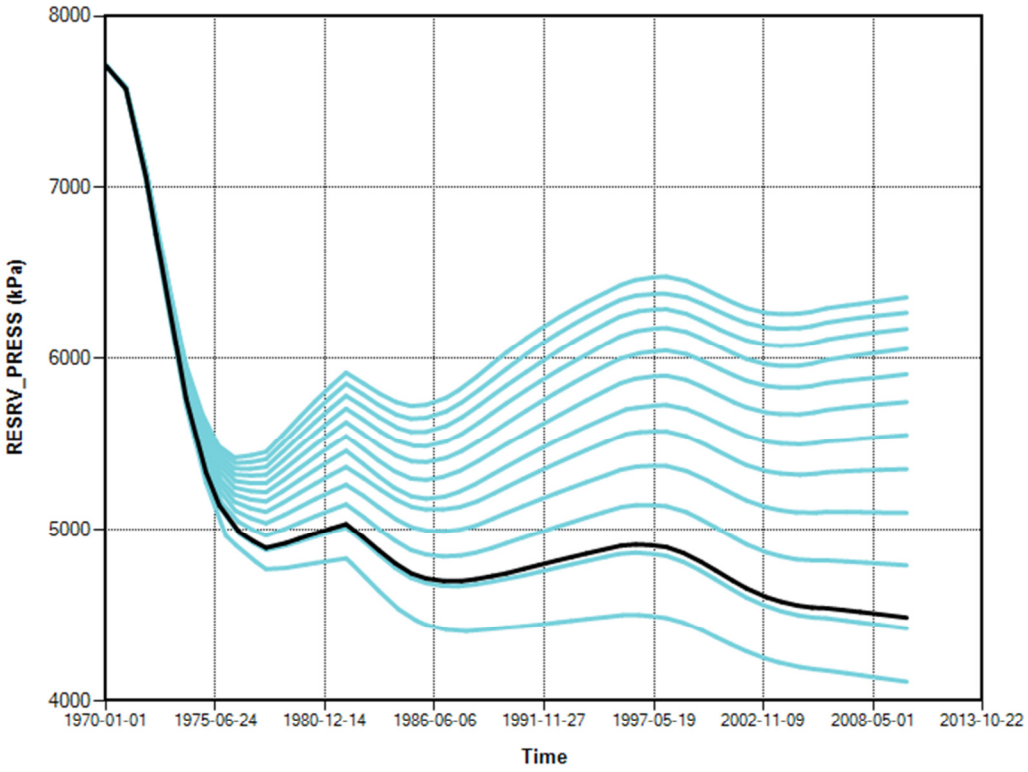

Figure 22 - Pressure history of the Messoyakha field as a pure gas field with aquifers of different strengths

If an active aquifer was present and supported the reservoir, the GWC would move toward the surface in time. In the case of the observed pressure history, an increase in the GWC level would have reached a depth of 770 m (2,525 ft), and the producing intervals of for existing Well (#2, 124, 139, and 161) would be below the GWC level and a rapid liquid loading would be observed. This did not occur in the actual production history; therefore, the presence of an active aquifer is not confirmed.

The total reservoir volume was also studied. Observed pressure behavior was confirmed only at the reservoir volume of 1.69 x 10^9 m^3 (60 x 10^9 SCF), corresponding

to a reserve value of 23.8 x 10^9 m^3 (840 x 10^9 SCF) which is close to the value obtained by field development engineers.

Because the pressure response achieved during the adaptation is in good agreement with the actual reservoir pressure behavior, reflecting real reservoir volume and the OGIP, the model is ready to be used for further study of pressure support mechanisms.

In the next chapter, we are going to discuss different methods that can be used to obtain the contribution of gas hydrate to overall production, thermodynamic behavior of the field, and pressure-support mechanisms.

CHAPTER IV

COMPARISON OF THE RESULTS OBTAINED IN THE DIFFERENT SOLUTION SCENARIOS

This chapter presents three calculation methods for determining gas hydrate contribution to overall production from the Messoyakha field. In addition, overall volume of water encroachment into the formation due to hydrate decomposition and temperature changes is considered.

The first calculation method is based on the assumption that the gas hydrate decomposition process can be substituted by adding an extra component (gas) into the reservoir by means of a set of gas-injection wells. The gas injected through these wells represents the gas obtained due to the hydrate decomposition.

Water is also a product of hydrate decomposition. In the second calculation method, a set of water- and gas-injection wells represents gas hydrate decomposition by means of simultaneous water and gas injection (SWAG). It was observed that this calculation method more accurately describes the decomposition process.

In the third calculation method, a non isothermal simulator was used to obtain the temperature changes in the field. The results obtained by this model were compared to the actual field temperature measurements.

The results obtained in each scenario are compared with each other as well as with actual field data.

4.1. Application of gas injection wells for pressure support study in the Messoyakha field

In similar settings, isothermal simulations require less CPU time than nonisothermal simulations. Isothermal methods can be used for history matching of pressure-support mechanisms in gas hydrate reservoirs with unknown original hydrate in-place and gas hydrate distributions. This simplification also enables one to calculate the gas hydrate contribution to the overall gas production, which can be used as a first approximation for input values of hydrate saturation for a non isothermal simulator.

One unit volume of hydrates delivers 164 unit volumes of gas after decomposition and 0.8 units volumes of water. The amount of gas that is being released is significantly contributing to pressure support.

Gas-injection wells were added to the reservoir model (Fig. 23). Gas injected into formation had exactly the same composition as a gas obtained due to methane hydrate decomposition.

The annual production from the field and individual production from each well remained unchanged. Reservoir pressure in the absence of the set of injection wells would have behaved as a volumetric gas reservoir.

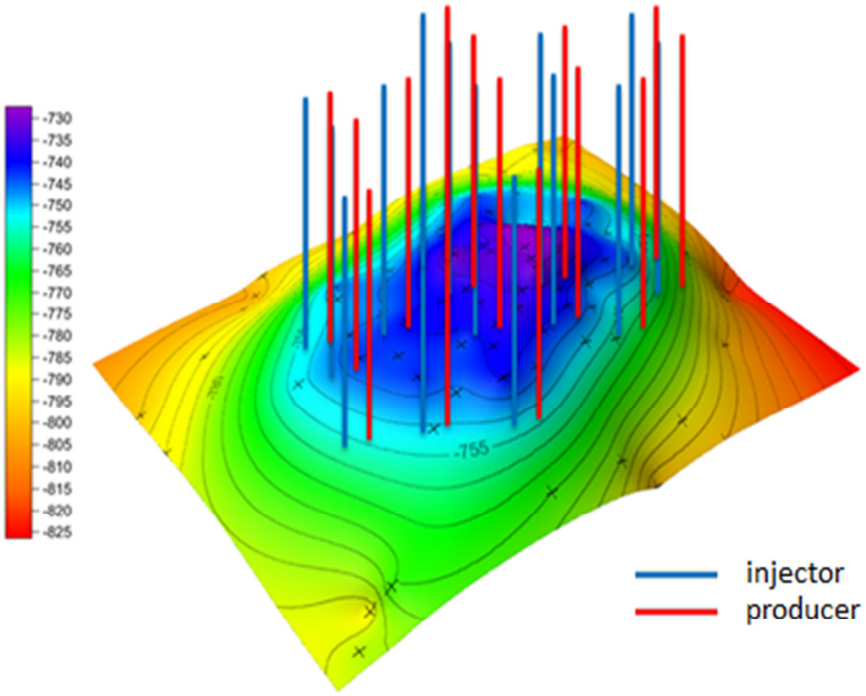

Figure 23 - Set of injection wells in the Messoyakha field installed for the first solution scenario

The injection rates of all the wells were automatically programmed to match the actual reservoir pressure. In this case, the volume of gas injected in the reservoir to provide pressure support in the simulation corresponds to the volume of gas obtained due to the decomposition of the hydrates. The amount of injected gas allows for determining the volume of hydrates to be decomposed, and the volume of water to be encroached into formation. The results obtained in the model were compared with the actual reservoir parameters. Fig. 24 represents the actual pressure behavior vs. pressure obtained by the model. As shown in the plot, the values predicted by our model closely follow the actual data with the highest perturbation of 5%.

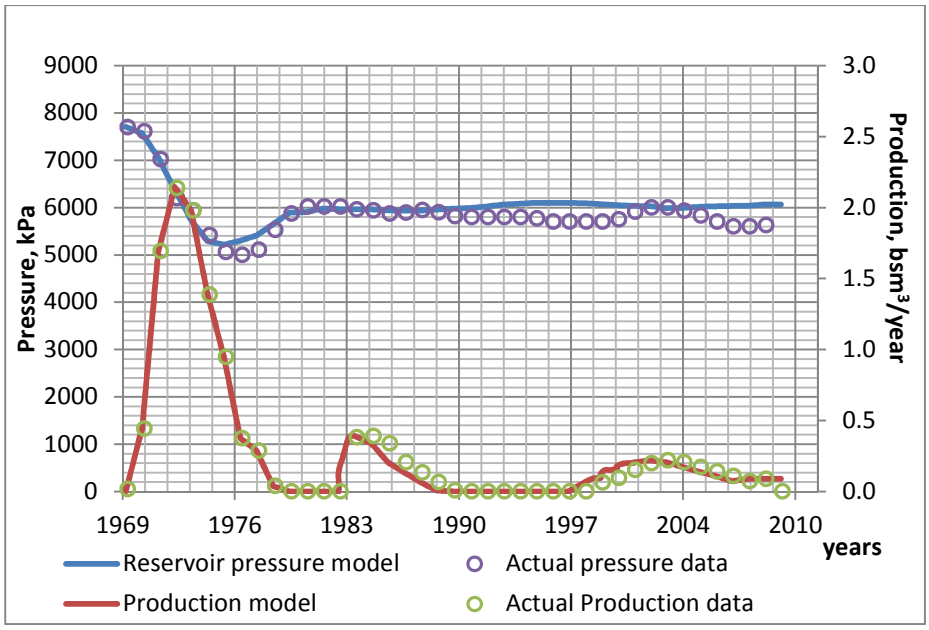

Figure 24 - History-matched pressure by the isothermal model

The volume of injected gas is shown in Fig. 25. This volume corresponds to the volume of gas obtained in the decomposition process. The cumulative gas production from the Messoyakha field on January1, 2012 was 12.9 x 10^9 m^3 (456 x 10^9 SCF) of gas, and according to the first-solution scenario, the volume of gas obtained due to hydrate decomposition is 7 x 10^9 m^3 (248 x 10^9 SCF).

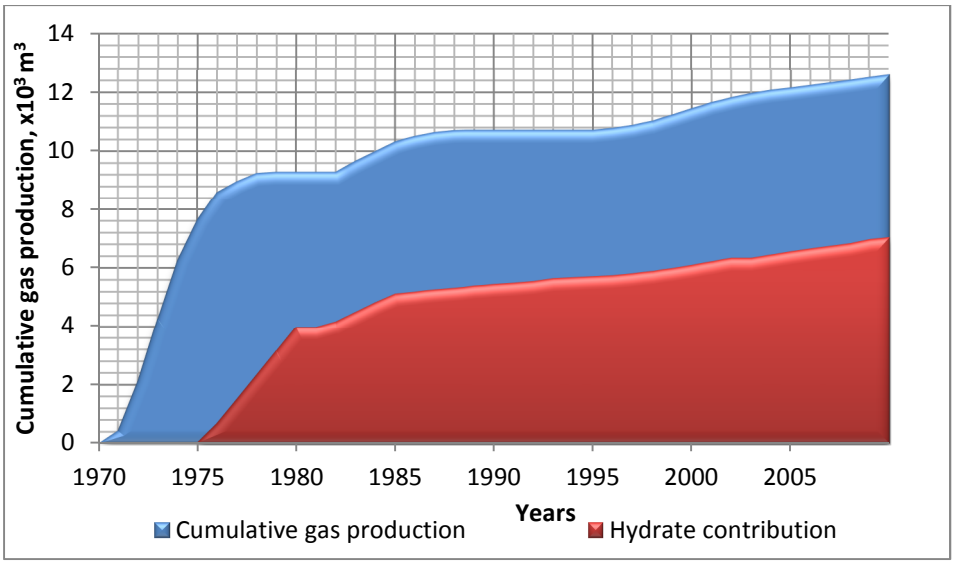

Figure 25 - Gas hydrate contribution to overall production

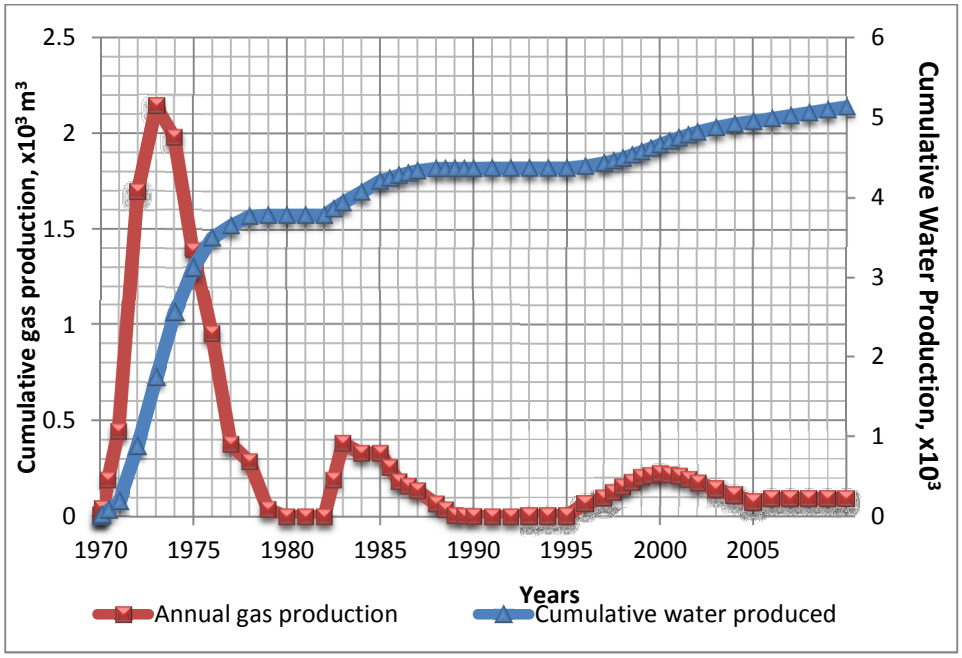

Figure 26 - The volume of water produced in the Messoyakha field

It is shown in Fig. 25 and 26 that the hydrate decomposition process does not begin until the pressure drops below the equilibrium pressure. The slope of the curve

corresponds to the rate of gas hydrate decomposition, which is caused, in this case, by the driving mechanism (draw down below equilibrium pressure). The slope of the curve that corresponds to the time prior to the first shut-in period of the field is the greatest. At that time, the pressure dropped below equilibrium by almost 1 MPa (147 psi). The slope then changes and corresponds to a lower drawdown pressure below the equilibrium point.

The cumulative amount of decomposed hydrate gas is defined by cumulative gas injected into the field. Thus, if there was a hydrate in the pores in the upper portion of the reservoir, the volume of the decomposed hydrate should be about 43 x 10^6 m^3 (1.518 x 10^9 $m^{3)}$, which corresponds to almost 7 x 10^9 m^3 (248 x 10^9 SCF) of gas obtained due to hydrate decomposition.

The volume of gas obtained due to decomposition and the total volume of gas produced from the Messoyakha field are shown in Fig. 25. VRR, defined by Dr. Moridis, shown in Fig. 27, is calculated by the following expression:

$$VRR = \frac{V_r}{V_p} = \frac{\int_0^t Q_r(t)dt}{\int_0^t Q_p(t)dt} \tag{11}$$

Grover et al. (2008) attempted to calculate the VRR values for one of the wells in the Messoyakha field. Calculations were performed for one well and only for the first several years of production. In this study, the VRR values were calculated for the entire field development history. These are the first values obtained for the contribution of hydrates to overall gas production from a gas hydrate field.

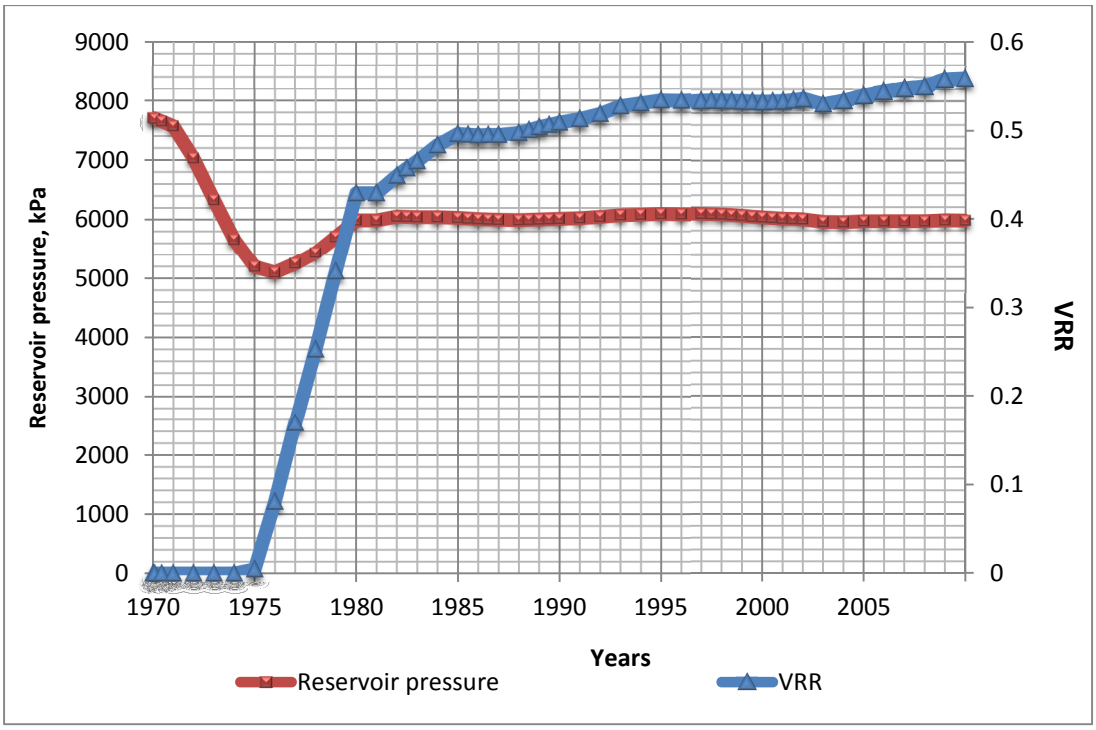

Figure 27 - Volume replenishment ratio

.

The overall contribution of gas due to hydrate decomposition is increasing due to the fact that the total volume of free gas in place is decreasing (Fig. 27). The final VRR value obtained in this study is 56%, meaning that 56% of the gas produced was obtained from gas hydrate decomposition.

The volume of water obtained from hydrate decomposition is 48 x 10^6 m^3, (1.694 x 10^9 SCF) which is three orders of magnitude greater than the value obtained in the field. The water produced in addition to the gas from the wells in the Messoyakha field were compared versus water obtained due to hydrate decomposition and are shown in Fig. 28. The volume of water obtained due to hydrate decomposition is significantly greater than the volume of water produced from the wells; therefore, water obtained due

to hydrate decomposition stays in the reservoir, contributing to additional pressure support and cannot be ignored.

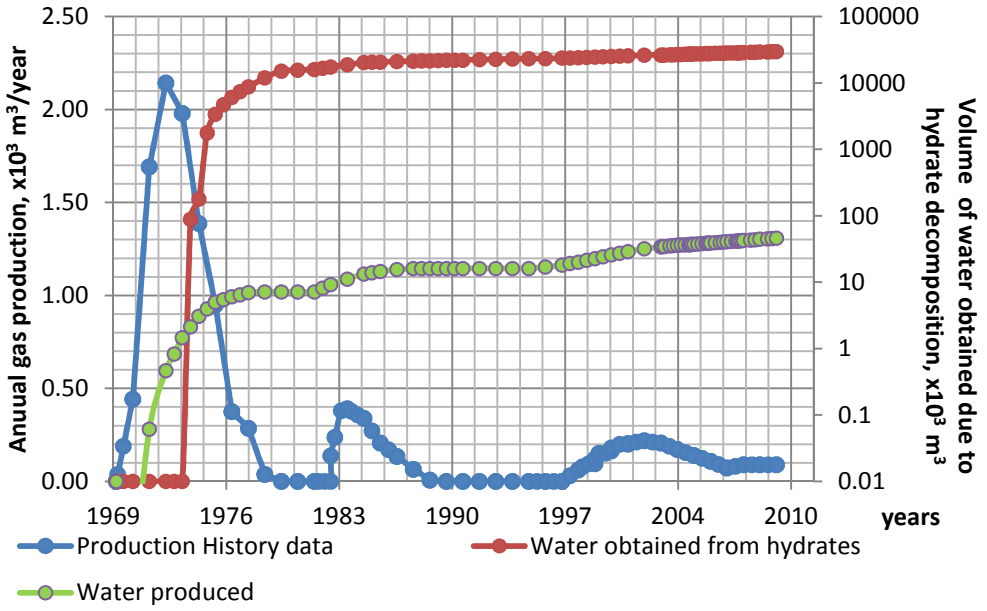

Figure 28 - Cumulative water encroachment into the formation and water produced from the reservoir

4.2. Application of simultaneous water and gas injection for pressure support study of the Messoyakha field

As shown in the previous study, the volume of water obtained in the decomposition process is significant and cannot be ignored in the pressure support calculations. Therefore, for a better description of the pressure behavior, a group of SWAG injection wells was implemented, injecting gas and water at a volumetric ratio of 1:208 (exactly corresponds to the ratio of water/gas in a gas hydrate). The results obtained during SWAG injection are noticeably different from those that were obtained by injecting a free gas (Fig. 29).

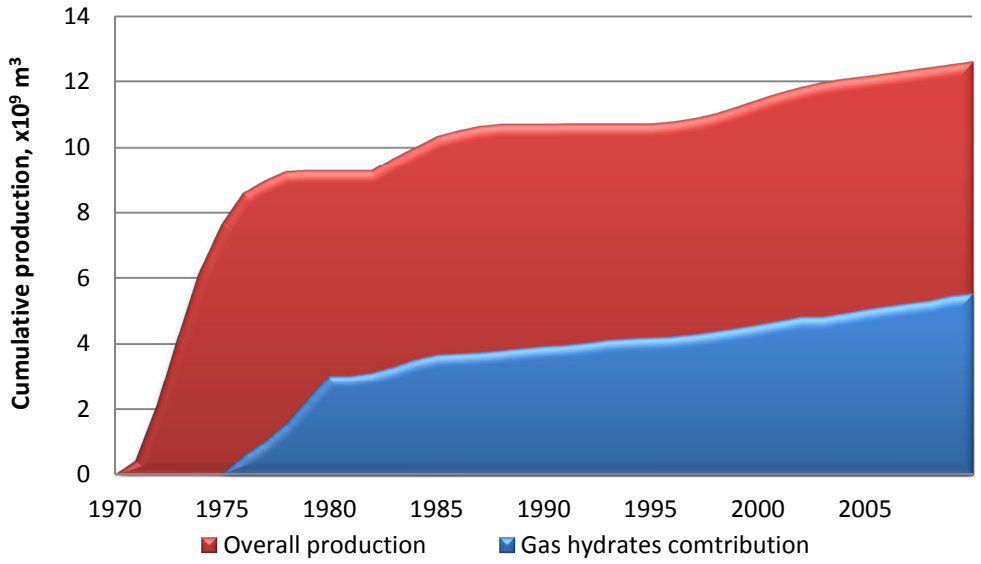

Figure 29 - Gas hydrate contribution to overall production while applying SWAG injection

The volume of gas injected into the formation is significantly less than the volume obtained during a pure gas-injection scenario. Water injected in the reservoir provides additional support for reservoir pressure; hence, less gas is required to obtain the actual pressure profile.

The contribution of gas hydrates in this case was only 5.4 x 10^9 m^3 (190 x 10^9 SCF), which is significantly less than the value obtained when pure gas was injected. Water provided additional support for the reservoir pressure.

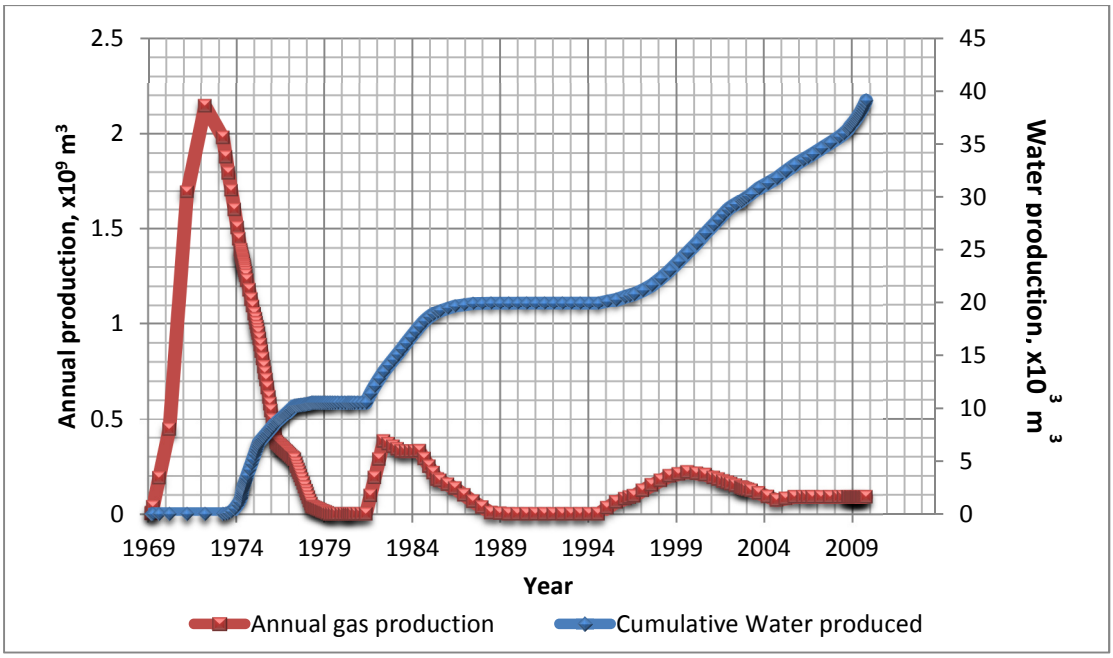

Figure 30 - The volume of water produced during SWAG injection

Because less gas is injected into the formation in this study compared to scenario 1, a lower value of VRR is obtained compared with pure gas injection. However, the volume of water produced, 40 x 10^3 m^3 (251 x 10^3 bbls), is significantly higher than the volume obtained in solution scenario 1, and corresponds to the volume obtained in the field, which was 48 x 10^3 m^3 (301 x 10^3 bbls) (Fig. 30).

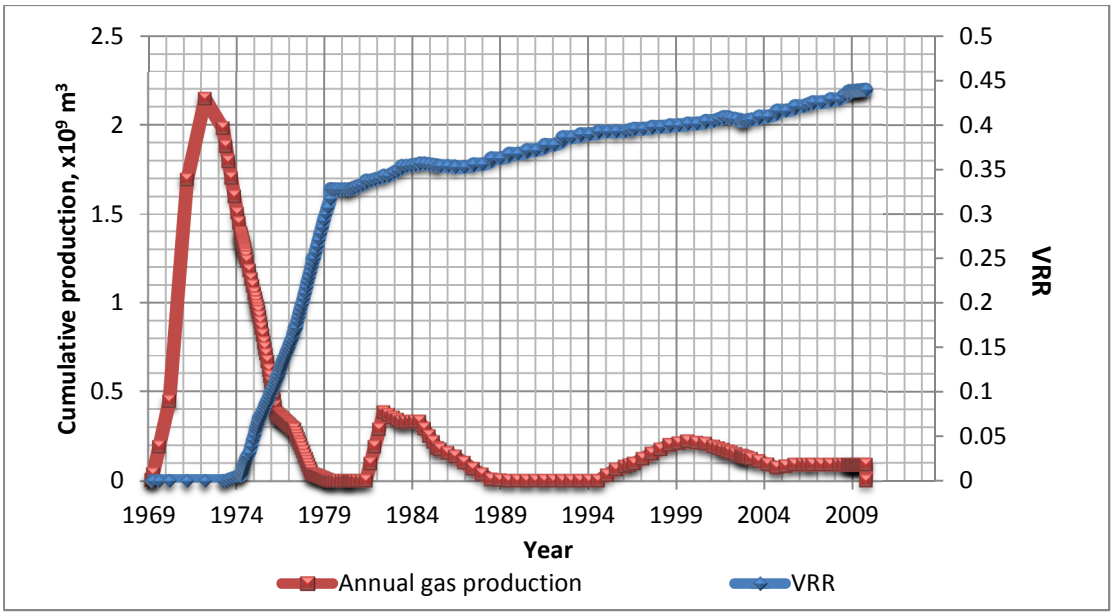

Figure 31 - VRR during SWAG injection

The volume of water encroaching into the formation is significant and has to be accurately included as a pressure-support mechanism, which was shown by a comparison of pressure support using a set of pure gas injection wells and SWAG injection. The difference in the volume of gas required to the support actual pressure history is 1.6 x 10^9 m^3 (57 x 10^9 SCF).

The overall contribution of gas obtained due to hydrate decomposition is increasing due to the fact that the total volume of free gas in place is decreasing as was observed in the previous study (Fig. 31). The final VRR value obtained in this study is 44%, meaning that 44% of the gas produced was obtained from gas hydrate decomposition. This value is a significantly lower value than obtained during the pure gas injection simulation due to the fact that partial pressure support is provided by the injected water.

4.3. Application of a nonisothermal simulator for the pressure support study in the Messoyakha field

Uncertainty in the position of the boundary between the free gas and hydrate phases, and hydrate saturation distribution in the hydrate stability zone complicates the process of obtaining a solution in the nonisothermal simulator. Several models of hydrate saturation distribution were created to study the pressure-support mechanism. The results obtained from the nonisothermal model are very similar to those that were obtained from the isothermal simulator with injection of water and gas. Including energy conservation into the calculation process allowed for obtaining temperature changes in the field.

The results obtained from the model were compared to actual reservoir parameters. Fig. 32 presents the actual pressure behavior and the pressure obtained with the model as well as production rates obtained by the model versus actual production rates. The difference in the values did not exceed 5%, except when the decomposition process was initiated. This deviation is most likely due to the inaccuracy of the decomposition kinetic model.

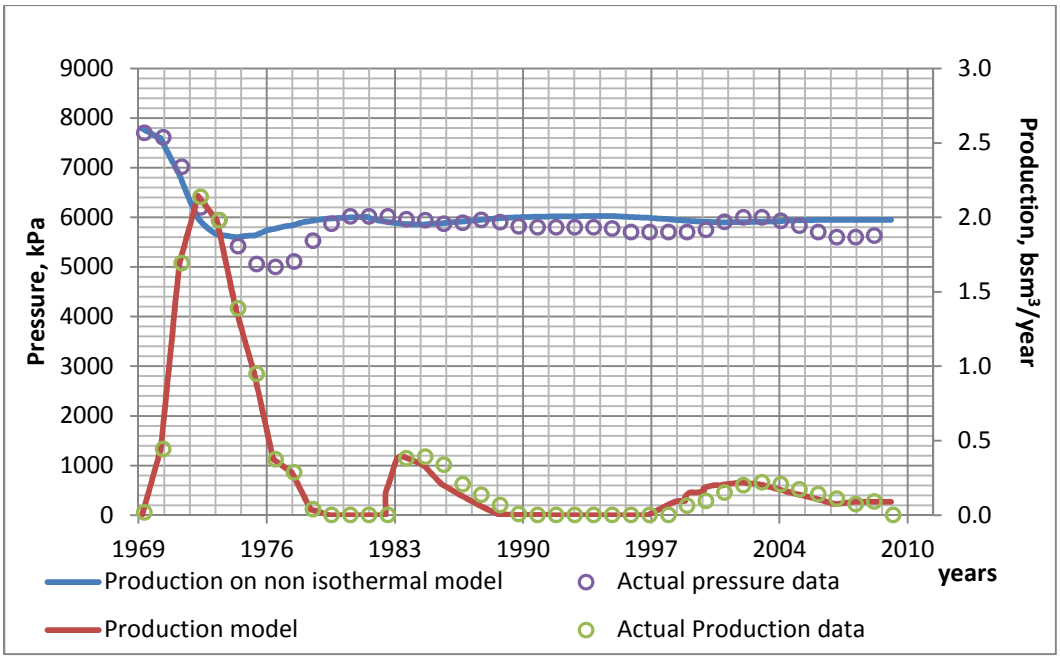

Figure 32 - Results of simulations obtained from the nonisothermal simulator

The volume of gas obtained due to hydrate decomposition is shown in Fig. 33. The cumulative production from the reservoir on January 1, 2012 is 12.9 x 10^9 m^3 (455 x 10^9 SCF) of gas, and according to the nonisothermal simulation, the volume of gas obtained due to hydrate decomposition is 5.4 x 10^9 m^3 (195 x 10^9 SCF) .

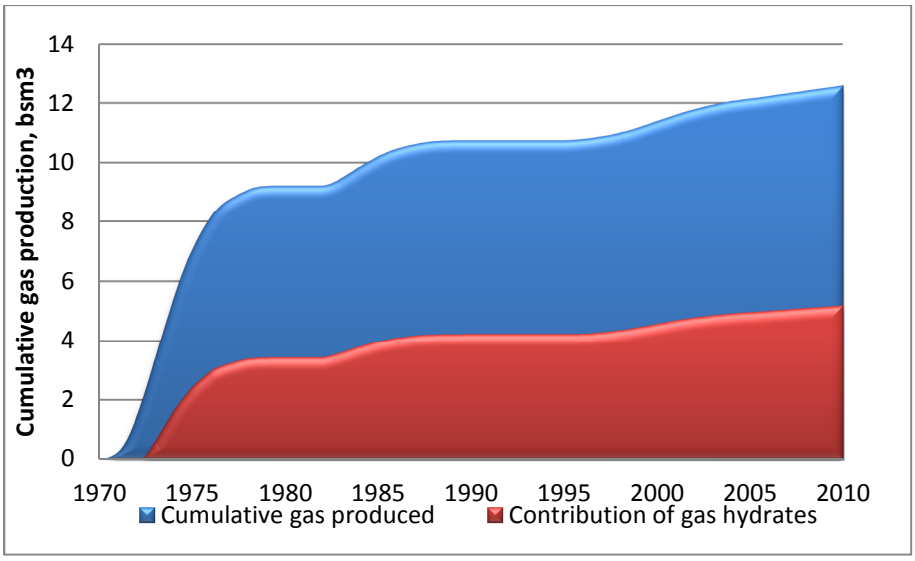

Figure 33 - Gas hydrate contribution to overall gas production from the Messoyakha field

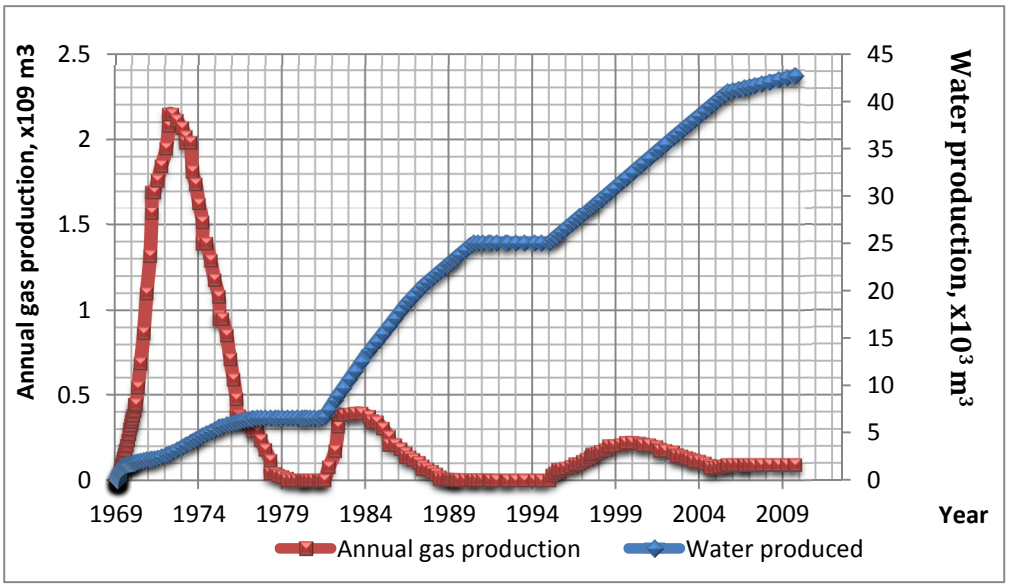

Figure 34 - Water production from the Messoyakha field obtained by the nonisothermal simulator

The volume of water obtained by solving the problem using the nonisothermal simulator adequately reflects the amount of fluid entering the reservoir due to hydrate

decomposition and was determined to be 44 x 10^3 m^3 (276 x 10^3 bbls) (Fig. 34). According to the results obtained from the model, the amount of water that encroached the formation due to hydrate decomposition is 48 x10^6 m^3 (301 x10^6 bbls). At the time, the volume of water extracted from the field amounted to approximately 49 x 10^3 m^3 (307 x10^3 bbls), which is less than 1% of the volume of water received in the reservoir due to the decomposition of hydrates. Water obtained due to hydrate decomposition remains in the reservoir, contributing to additional pressure support.

In Fig. 35, the volume of hydrate in place for one of the scenarios is shown during the time of development of the Messoyakha field. The initial shut-in period did not stop the decomposition process. After all of the wells were shut-in, the difference between equilibrium and average reservoir pressures was still causing hydrates to decompose. However, when the field was shut-in at a pressure near equilibrium, the hydrates volume remains unchanged.

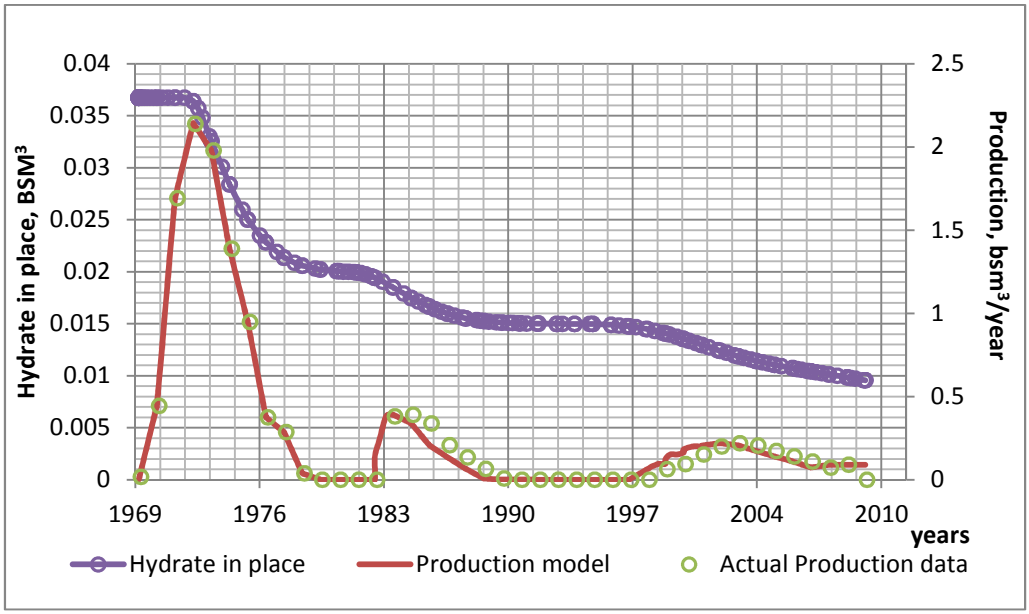

Figure 35 - Hydrates in-place

Several hypotheses have been considered for the hydrate distribution, but regardless of the total volume of hydrate in the deposit, the amount of decomposing hydrate is almost independent of the overall hydrate initially in place. This condition is most likely due to the fact that the decomposition of hydrate is taking place at the boundary and not in the bulk volume. Even at very low-hydrate saturations, the reservoir rocks are completely impermeable to pressure-front propagation. Thus, the decomposition takes place only at the boundary of the hydrate/free-gas interface. The initial hydrate can only affect the residual gas reserves in the field.

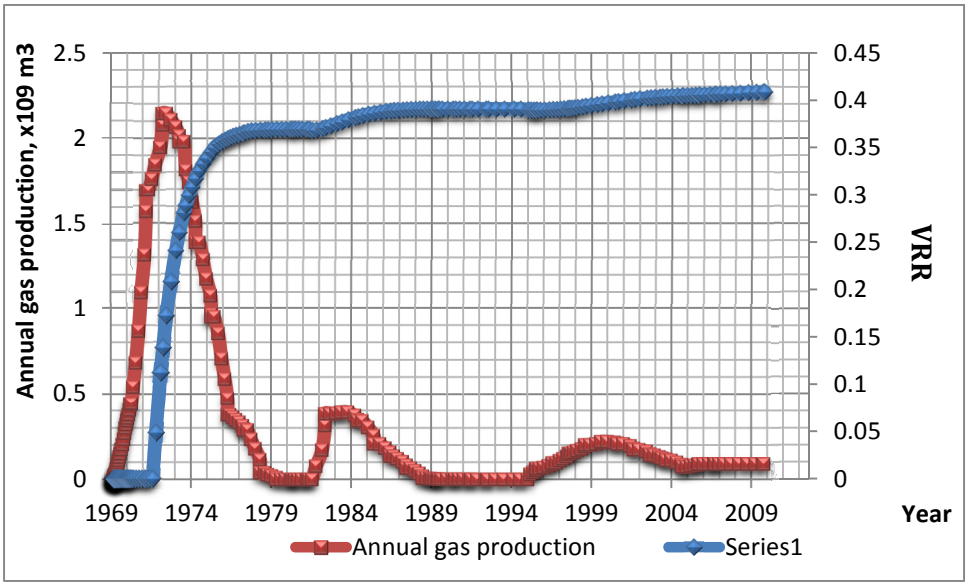

Figure 36 - VRR obtained by the nonisothermal simulator

The overall contribution of gas obtained due to hydrate decomposition is increasing due to the fact that the total volume of free gas in place is decreasing (Fig. 36). The final VRR value obtained in this study is 41%, which means that 41% of the gas produced was obtained from gas hydrate decomposition.

4.4. Comparison of different calculation scenarios

The next step of this study was to compare different calculation techniques and determine the benefits and drawbacks of each of them. A comparison of VRR values obtained by different calculation methods is presented in Fig. 37. The green line represents the VRR for isothermal simulation with only gas injection. The VRR is much higher than any others due to the fact that it does not take into account water obtained due to hydrate decomposition, which is significant.

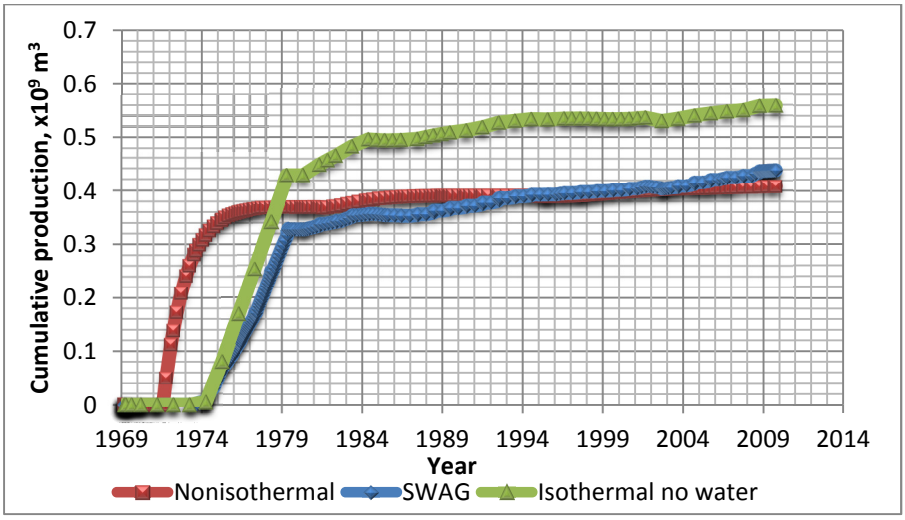

Figure 37 - VRR obtained by different methods

The values obtained in the SWAG injection scenario and by the nonisothermal simulator are similar; i.e., 44 and 41%, respectively. With the nonisothermal simulator, decomposition begins earlier than in previous solution scenarios. The same result was also observed on the average pressure curve.

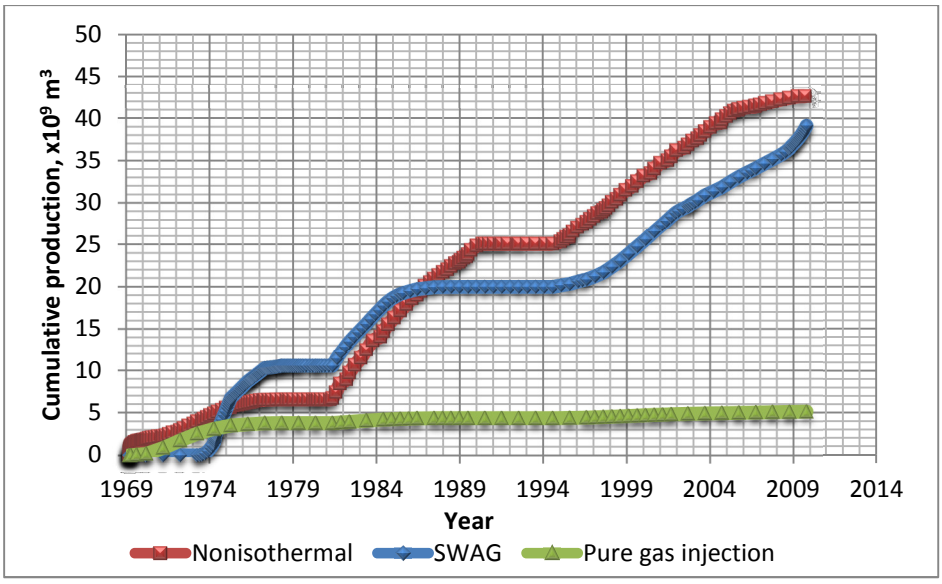

Figure 38 - Water encroachment into the formation obtained by different methods

The water production in the pure gas-injection scenario is very small (Fig. 38). The only source of water in this case is the formation water that is able to flow above the irreducible water saturation. The values obtained during the SWAG injection and non isothermal scenario are much higher because of the additional water source due to hydrate decomposition. The volume of water obtained by the nonisothermal simulator is higher at the beginning because the decomposition of hydrates begins close to the wellbore, and water can reach the wellbore almost immediately. In comparison, during the SWAG scenario, it takes more time for the injected water to reach the producing wells. Also, injection does not start until the pressure dropped below the equilibrium point.

Such a small amount of water produced in the field is likely related to the magnitude of drawdown pressure that was set up in the wells. The reservoir is a very unconsolidated sandstone and confines the values of drawdown pressure that can be

placed in the well. Another suggestion is that the decomposition of hydrate takes place far from the wells and water is not able to reach the wellbore under such a small drawdown pressure value. For example, the Mallik well during the test was producing water in the amount of 35 liters/10^3 of water/1000 m^3 of gas (0.3 bbl of water/ 35MSCF), but the drawdown pressure at the well was several MPa (Table 8).

Table 8 - Comparison of Well Productivity From The Messoyakha and Mallik fields

Mallik 2007 Test	Mallik 2008 Test	Messoyakha, Average	
2L-38	2L-38	Well #121	Well#1
Perforated only in hydrate zone, net pay 12 m		Perforated only in hydrate zone, net pay 11 m	
1000–2000 m^3/D (35–70MSCFD)	2000–3000 m^3/D (70–105 MSCFD)	15800 m^3/D (558 MSCFD)	28300 m^3/D (1,000 MSCFD)

When working with small levels (0.5-1 MPa) of drawdown pressure, the amount of water extracted from the deposit is very small (less than 1% of water obtained from hydrate decomposition). Therefore, water from the hydrate decomposition remains in the deposit. This reasoning might be an argument opposing the theory that the absence of gas hydrates in the Messoyakha deposit results in a lack of water.

4.5. Thermodynamic behavior of the Messoyakha field

The process of hydrate decomposition is an endothermic reaction; it progresses with the absorption of heat. The temperature of the decomposition area decreases with

time as well as average field temperature if the pressure is less than the equilibrium reservoir pressure.

Thermodynamic behavior was studied only on a nonisothermal model. The observed temperature behavior was in close agreement with the values reported in the field. The average reservoir field temperature is shown in Fig. 39. Initial average reservoir temperature was approximately 9.8°C (50 F). The initial drop in reservoir temperature is due to the Joule-Thomson effect and hydrate decomposition around the wellbores. The sharpest decline in temperature was observed during the largest production rates from the field, when the active process of decomposition began. Each increase in the production rates from the field leads to formation cooling, which should be taken into account when developing any gas hydrate field. The formation cooling preserves hydrate from decomposition under the same drawdown principle, which results in either formation heating or decreasing the wellbore pressure to an even lower value.

Temperature behavior of the Messoyakha field is crucial, because it defines the beginning and the end of the decomposition as well as decomposition area. The temperature in the vicinity of the wellbore was calculated and compared to the field data. The graph in Fig. 39 shows the behavior of the field temperature in the vicinity of the Well #162 and #163. Average reservoir temperature is decreasing due to the endothermic reaction of hydrate decomposition.

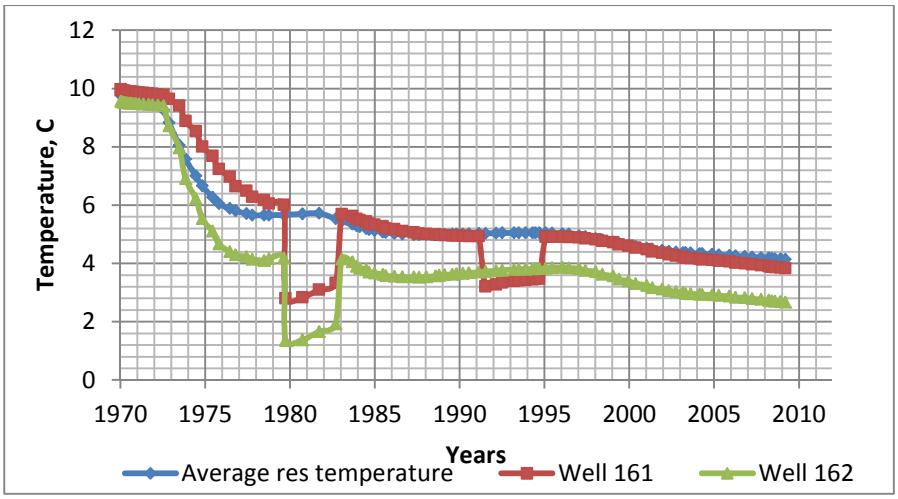

Figure 39 - Temperature behavior in Wells #162 and #161

The overall trend of the temperature for both of these wells repeats the trend of the average reservoir pressure; however, the temperature behavior is different during the shut-in periods. Well #162 was shut in only one time, so it has only one sudden pressure drop. On the other hand, Well #161 was shut in twice and we can observe two decreases in pressure. The explanation for this sharp drop is that while the well is producing, the inflow of warm fluid from the free-gas zone keeps the well temperature at high level. As soon as the well is shut-in, there is no warm fluid inflow and this zone is cooling due to the continuing reaction of hydrate decomposition in the areas surrounding the zone. As soon as the well is placed back on production, the pressure profiles increase and return to the average reservoir level because of the warm fluid inflow. The process of formation temperature restoration is rather slow as shown on the Fig. 39 plot during the shut-in periods. It is critical to heat the area surrounding the wellbore during field development, especially in overcooled gas hydrate formations. Shut-in periods will be

very dangerous while producing gas hydrate wells. For that reason, inhibitor injection should be completed prior to shut in.

In this study, we compared different development scenarios for the Messoyakha field. The endothermic character of the gas hydrate decomposition process reduces the production rate. To show the influence of temperature influence and endothermic reaction of hydrate desomposition, a nonisothermal model was run to predict reservoir behavior to 2030 using two scenarios. In the first scenario, temperature changes in the field occurred during the field's development. In the second scenario, temperature changes were disabled.

The results of the calculations are presented in Fig. 40. Higher drawdown pressure is required for hydrate decomposition on the nonisothermal simulator to initiate the decomposition process due to cooling of the reservoir. The difference in the amount of hydrates in place is significant at the end of the specified period. In the isothermal scenario, no hydrate remained by 2030, and reservoir pressure was 5.5 MPa (805 psi). In the nonisothermal scenario, almost 25% of initial hydrate remained in place (25×10^6 m^3 or 883×10^6 SCF), and the reservoir pressure was still at equilibrium for the Messoyakha field conditions (approximately 6.0 MPa or 879 psi). The formation cooling can be a significant problem while developing overcooled gas hydrate formations. Decomposition zone heating or any other alternative ways of restoring reservoir temperature should be applied in this case.

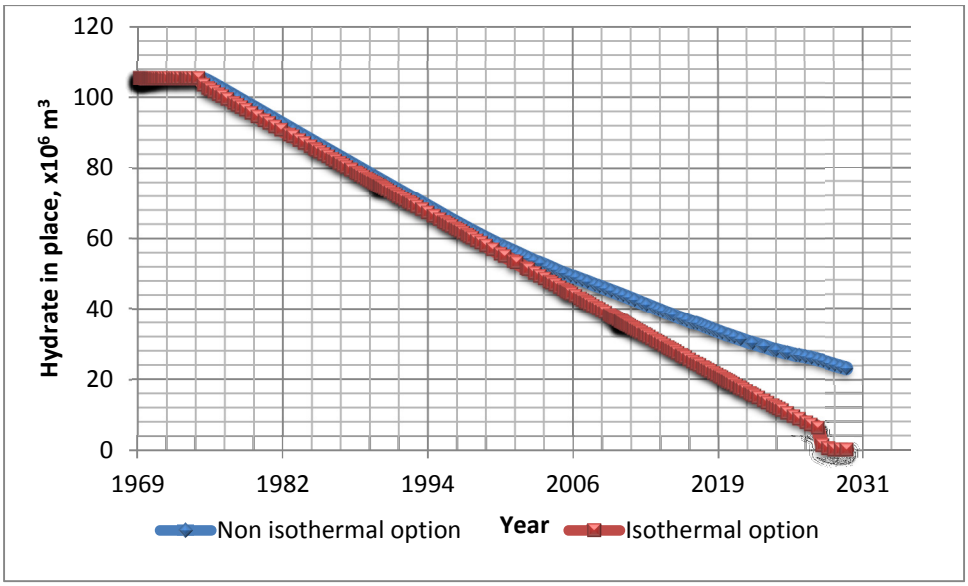

Figure 40 - Hydrate in place in time for the isothermal and nonisothermal scenarios

As a result of the simulations, the potential areas of where hydrate could be preserved were obtained for different periods of time. According to the calculations and for a number of reasons, the bulk of the hydrate can be preserved in the upper portion of the anticline with the high density of the wells. First, this portion of the reservoir is the coolest; i.e., the initial temperature is 8°C (46 F). Second, the average reservoir pressure is the lowest in central part of anticline and the active process of hydrate decomposition cooled the formation very quickly (Fig. 41–43). The reservoir edges can still preserve hydrate due to the fact that the average reservoir pressure in this area remains high. The area between the edge and the central portion of the reservoir is where most of the active hydrate decomposition occurs. Formation cooling in this area can be easily restored by heat inflow from the surroundings due to the small drawdown.

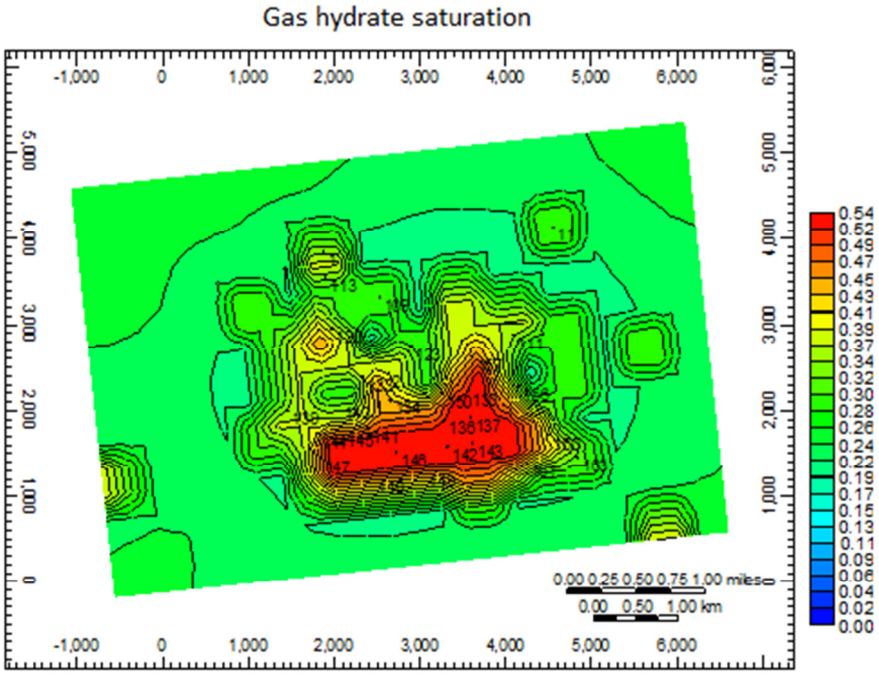

Figure 41 - Gas hydrate saturation distribution in the top layer on January 1, 1975

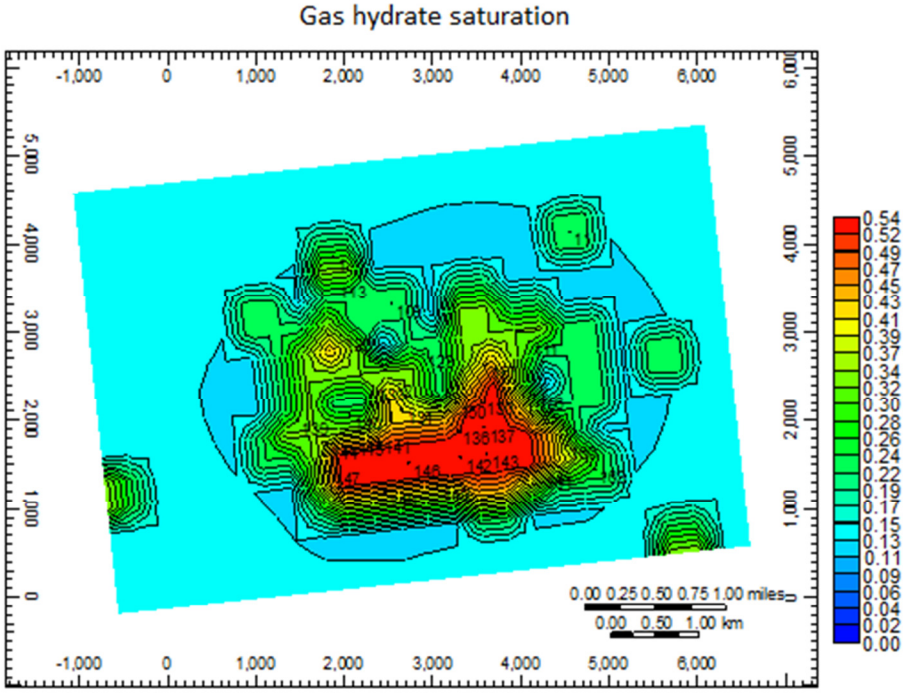

Figure 42 - Gas hydrate saturation distribution in the top layer on January 1, 1988

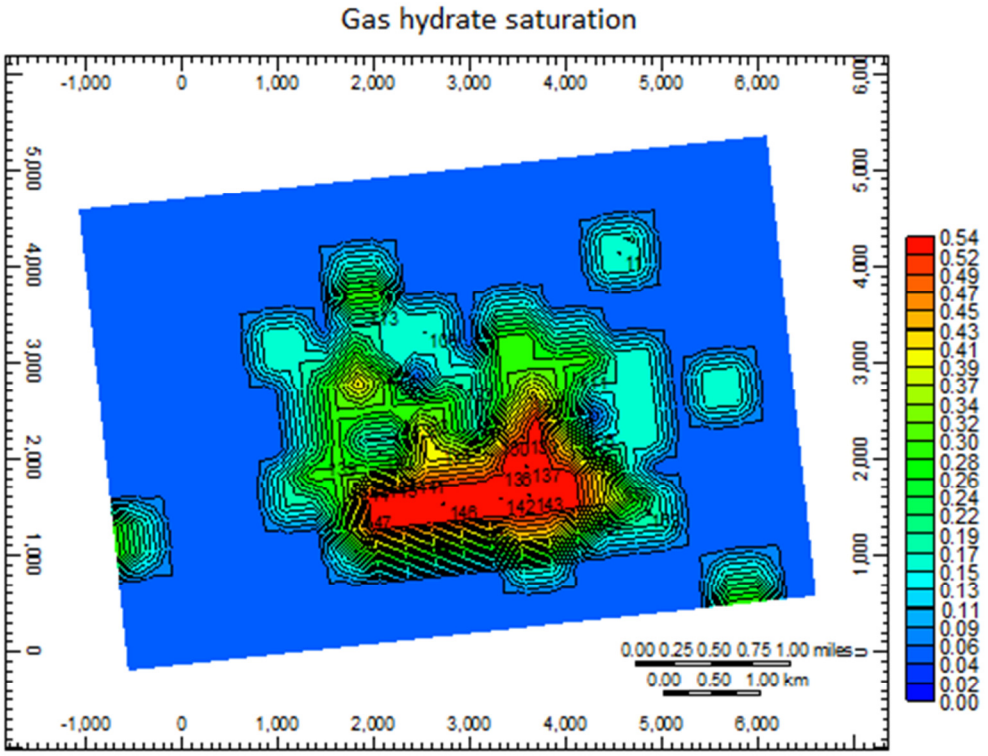

Figure 43 - Gas hydrate saturation distribution in the top layer on Januray 1, 2010

The calculation results are presented in Fig. 44. As was noted previously, most of the water obtained due to hydrate decomposition remained in the reservoir to support the reservoir pressure. A sharp increase in water saturation was observed on the border of the free gas and gas hydrate, leading to a formation with a thick water layer. Such a layer was observed in the field. The water saturation distribution in time is also shown in Fig. 44. The initial average water saturation in the hydrate layer was 50%, and the initial average water saturation in the free-gas layer was 40%. After decomposition of the hydrate, water saturation in the pores increases to 92%. This water moves downward to the free-gas zone and forms a water layer.

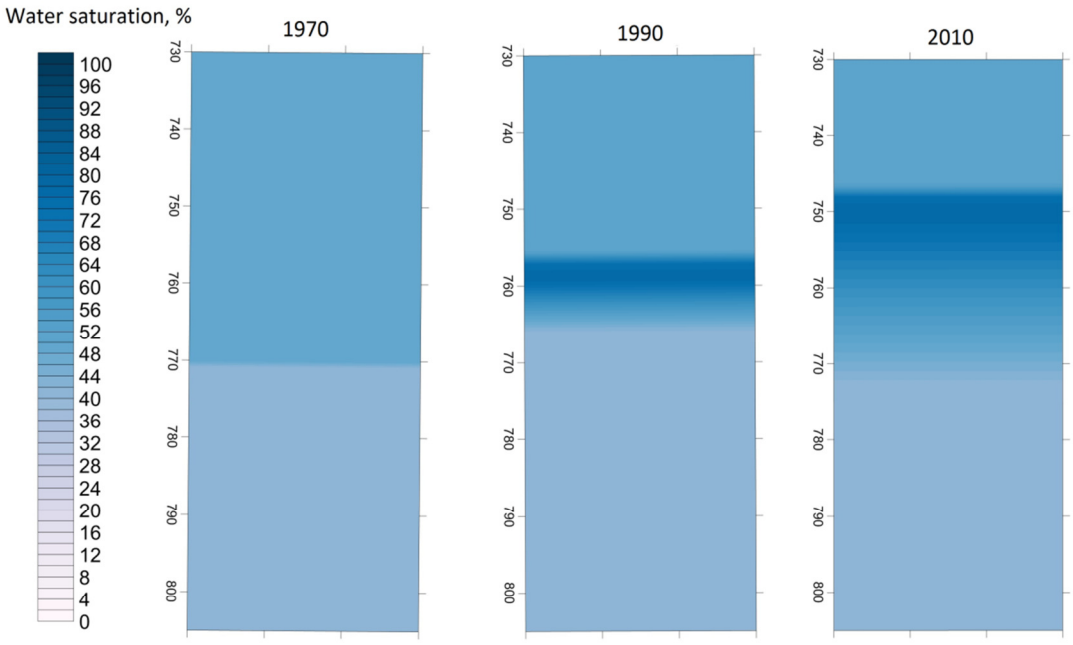

Figure 44 - Water saturation distribution at different times

Formation of thick water layer is a very important observation because this layer could be the main reason for the liquid loading in the producing wells in the Messoyakha field. This kind of behavior was not obtained on the isothermal simulator during the calibration procedure because there was no water in the reservoir due to hydrate decomposition. Most of the wells were designed for much smaller amounts of water in the reservoir, so the wells were not able to handle excessive water production and were shut in. Additional hydrate formation plugged these wells. Production restoration from these wells is possible by means of inhibitor injection or heating; however, this could be a possible problem for all of the wells in the permafrost and offshore.

CHAPTER V

CONCLUSIONS

- Although the presence of gas hydrates in the Messoyakha field was previously debated, this thesis proves the presence of gas hydrates in the reservoir. The contribution of gas hydrate in the cumulative gas production is 41%; and 5.4 x 10^9 m^3 of gas was produced from hydrates. The initial volume of gas hydrates in the field was determined to be 105 x 10^6 m^3. Original gas in place, both in free and solid state, is in the range of 35 to 42 x 10^9 m^3, and the current recovery value is slightly greater than 30%. The areas of possible current hydrates preservation were identified.
- Thermal effect of hydrate decomposition as well as thermodynamic behavior of the field were examined during the study, comparing the temperature behavior of the layer to the field measurements. It was shown that the observed pressure drop could be achieved only by hydrate decomposition not due to the Joule – Thomson effect. The study of formation temperature in the Messoyakha field showed that the it did not remain constant. The reservoir-pressure fluctuations are due to the self- preservation property of gas hydrates. Such fluctuations can be used to prove the presence of gas hydrates.
- The amount of water obtained due to hydrate decomposition is 45 x 10^6 m^3. The amount of water produced at the reservoir is 49 x 10^3 m^3, which is less than 1% of the total water obtained by means of decomposition. The volume of water encroaching into the reservoir due to hydrate decomposition is significant and should be considered as one of the pressure-support mechanisms.

- Even though there were numerous oil features of the reservoir, it was shown that there is currently no oil rim. An additional 170 x 10^6 m^3 (1491 x 10^6 STB) of oil could have been produced from the Messoyakha deposit; However, this oil might be found in nearby traps. With a 25% recovery efficiency and an oil market price of \$400/ m^3 (80 \$/bbl), the potential loss of revenue from the crude oil will exceed \$20 x 10^9.
- Potential areas of gas hydrate decomposition and preservation were determined. It has been shown that the highest concentration of hydrates is in the upper portion of the formation and at the edge of the anticline.
- The formation of a thick, unstable water layer on the boundary between the hydrate and free-gas layers was observed using simulation and confirmed by field data.
- The most important problems when developing gas-hydrate fields are: wellbore stability, water production from the wells, prevention of secondary hydrate formation, self-preservation of hydrates, and formation cooling, which requires formation heating or very low production rates.
- While developing gas hydrate fields in unconsolidated formations under low-drawdown conditions, high-water production rates should not be expected. The water produced at the surface is less than 1% of the water retained in the reservoir.
- Pressure does not remain constant in the reservoir while developing a gas hydrate field due to hydrate dissociation.

- While developing gas-hydrate deposits under high-drawdown pressure, greater water production rates should be expected, resulting in liquid loading. Furthermore, artificial water lift may be required for continuation of production.
- The only way to successfully develop gas-hydrate resources is through active exploration and production. A number of fields are ready to be developed.

REFERENCES

Bogatirenko, S., Sapir, Beniyaminovich. 1977. Determination of gas hydrate saturation of Senoman formation in Messoyakha reservoir. *Development and Exploitation of Gas and Gas Condensate Fields* **5**:10-16.

Collett, T.S. 1992. Geologic Comparison of the Prudhoe Bay - Kuparuk River (U.S.A.) and Messoyakha (U.S.S.R.) Gas Hydrate Accumulations. Paper SPE 00024469 presented at 01/01/1992.

Collett, T.S., Boswell, R., Lee, M.W. et al. 2012. Evaluation of Long-Term Gas-Hydrate-Production Testing Locations on the Alaska North Slope. *SPE Reservoir Evaluation & Engineering* **15** (2): pp. 243-264. SPE-155504-PA. doi: 10.2118/155504-pa.

Collett, T.S., and Ginsburg, G.D. 1997. Gas Hydrates In the Messoyakha Gas Field of the West Siberian Basin - A Re-Examination of the Geologic Evidence. Paper SPE ISOPE-I-97-017 presented at 01 Jan 1997.

DOE, E. 2011. Annual Energy Outlook 2011 projected to 2035. *EIA DOE* **1**.

Ertekin, T., Abou-Kassem, J.H., and King, G.R. 2001. *Basic Applied Reservoir Simulation*. SPE Textbook Series. Richardson, TX.

Filatov, K., Laperdin, Smirnov, Pletneva, Promzeleva, Mulyavin. 2008. Field-Geological Features of Messoyakhsky Gas Hydrate Deposit. Hypotheses and Facts. *Drilling and Oil* **07-08/2008**: 23-27.

Gaddipati, M. 2008. Code comparison of Methane Hydrate Reservoir Simulators using CMG STARS., Morgantown, West Virginia: 21-65.

Grover, T., Holditch, S.A., and Moridis, G. 2008. Analysis of Reservoir Performance of Messoyakha Gas Hydrate Field. Paper SPE ISOPE-I-08-399 presented at 01 Jan 2008.

Hammerschmidt, E.G. 1934. Formation of gas hydrates in natural gas transmission lines. *Industrial and Engineering Chemistry* **26(8)**: 851-855.

Jha, A.K., Bansal, G., Joshi, A. et al. 2012. Will Gas Hydrate Lying On Oceanic Floors In India Solve Its Energy Problem? A Futuristic Approach. Paper SPE SPE-152471-MS presented at SPE Europec/EAGE Annual Conference, Copenhagen, Denmark, 4-7 June 2012. doi: 10.2118/152471-ms.

Krason, J.A.N. 2000. Messoyakha Gas Field (W. Siberia): A Model for Development of the Methane Hydrate Deposits of Mackenzie Delta. *Annals of the New York*

Academy of Sciences **912** (1): 173-188. doi: 10.1111/j.1749-6632.2000.tb06771.x: 173-185

Kurihara, M., Sato, A., Funatsu, K. et al. 2010. Analysis of Production Data for 2007/2008 Mallik Gas Hydrate Production Tests in Canada. Paper SPE SPE-132155-MS presented at International Oil and Gas Conference and Exhibition in China, Beijing, China, 8-10 June 2010. doi: 10.2118/132155-ms.

Makogon, Y.F. 1965. A gas hydrate formation in the gas saturated layers under low temperature. *Gas Industry* **5**: 14-15

Makogon, Y.F. 1966. Specialities of exploitation of the natural gas hydrate fields in permafrost conditions. *VNIIGAZPROM* **11(4)**: 1-12.

Makogon, Y.F. 1981. *Hydrates of Natural Gases*. Tulsa, OK: PennWell. ISBN.

Makogon, Y.F. 1984. Production from Natural Gas hydrate deposits. *Gazovaya Promishlennost* **10**: 24-26.

Makogon, Y.F. 1997. *Hydrates of Hydrocarbons*. Tulsa, OK: PennWell. ISBN.

Makogon, Y.F. 2010. Natural gashydrates – A promising source of energy. *Journal of Natural Gas Science and Engineering* **2** (1): 49-59.

Manohar Gaddipati, B.J.A. 2012. 3D Reservoir Modeling of Depressurization-Induced Gas Production from Gas Hydrate Reservoirs at the Walker Ridge Site, Northern Gulf of Mexico. Paper SPE OTC-23582-MS presented at Offshore Technology Conference, Houston, Texas, USA, - 2012. doi: 10.4043/23582-ms.

Matsumoto, R. 2002. Comparison of Marine and Permafrost Gas Hydrates: Examples from Nankai Trough and Mackenzie Delta. . *Proceedings of the Forth International Conference on Gas Hydrates, Yokohama*.

Rajnauth, J.J. 2012. Is It Time to Focus on Unconventional Resources? Paper SPE SPE-158654-MS presented at SPETT 2012 Energy Conference and Exhibition, Port-of-Spain, Trinidad, 11-13 June 2012. doi: 10.2118/158654-ms.

Rutqvist J., M.G.J., Grover T., and Collett T. . 2009. Geomechanical response of permafrost-associated hydrate deposits to depressurization-induced gas production. *Journal of Petroleum Science and Engineering* **67**: 1-12.

Schebetov, A.V. 2008. Forecasting methods of gas hydrate fields development efficiency. *PhD thesis, Gubkin Russian State University of Oil and Gas*.: 25-60

Schoderbek, D. 2011. ConocoPhillips Gas Hydrate Production Test, Progress Report Second Half 2011. *Oil and Natural Gas Technology*. doi: DE-NT0006553: 10-44

Schoderbek, D. 2012. ConocoPhillips Gas Hydrate Production Test, Progress Report First Half 2012. *Oil and Natural Gas Technology*. doi: DE-NT0006553: 8-41

Tabatabaie, S.H., and Pooladi-Darvish, M. 2012. Hydrate Decomposition and Its Material Balance in a Volumetric Tilted Hydrate-Capped Gas Reservoir by Method of Depressurization. *SPE Reservoir Evaluation & Engineering* **15** (4): pp. 410-422. SPE-137610-PA. doi: 10.2118/137610-pa.

APPENDIX A

Overview

The equations are the result of the expressing all the relevant physical phenomena in mathematical form. There is one conservation equation for each chemical component for which a separate accounting is desired, along with some equations describing phase equilibrium between phases. There exist a set of these equations for each region of interest, which is usually a discretized grid block. Lastly, there is an equation describing the operating conditions of each injection and production well (Gaddipati 2008).

Conservation Equations

A conservation equation is constructed for each component (Ertekin 2001). All conservation equations are based on a region of interest (grid block) where

Rate of change of accumulation = [net rate of inflow from adjacent regions] + **A.1**

[net rate of addition from sources and sinks]

Accumulation terms

The total gross volume of a grid block may be composed of the following

V_r – *rock matrix*

V_s – *solid component (hydrate)*

V_w – *water or aqueous phase (o)*

V_g – *gaseous phase (g)*

V_o – *oil phase (o)*

The total (gross, bulk) volume is:

$$V = V_r + V_s + V_w + V_g + V_o \quad \textbf{A.2}$$

The fluid volume is

$$V_f = V_w + V_g + V_o \quad \textbf{A.3}$$

The void volume is

$$V_v = V_s + V_f \quad \textbf{A.4}$$

Porosity is defined as

$$\varphi = \frac{V_V}{V} \quad \textbf{A.5}$$

Saturations are defined as

$$S_w = V_w / V_f \quad \textbf{A.6}$$

$$S_o = V_o / V_f$$

$$S_g = V_g / V_f$$

$$S_w + S_o + S_g = 1$$

Flow terms

Solid components (hydrates) do not have flow terms. The flow term of flowing component I between two regions is:

$$T_w \rho_w w_i \Delta\Phi_w + T_g \rho_g y_i \Delta\Phi_g + \phi D_{wi} \rho_w \Delta w_i + \phi D_{gi} \rho_g \Delta y_i$$

The flow term of the energy between two regions is

$$\rho_w H_w V_w + \rho_g H_g V_g + k\Delta T$$

The volumetric flow rates are

$$v_j = T\left(\frac{k_{rj}}{\mu_j r_j}\right)\Delta\Phi, j = w, g \quad \textbf{A.9}$$

The phase transmissibility is T_j:

$$T_j = T\left(\frac{k_{rj}}{\mu_j r_j}\right), j = w, g \quad \textbf{A.10}$$

Well source/sink terms

Well source and sink term for flowing component *i* is:

$$\rho_w q_{wk} w_i + \rho_g q_{gk} y_i \quad \textbf{A.11}$$

Solid components do not have well terms

The well term source and sink for energy

$$\rho_w q_{wk} H_w + \rho_g q_{gk} H_g \quad \textbf{A.12}$$

The well phase rates for the layer k are:

$$q_{jk} = I_{jk}(p_{wfk} - p_k) \quad j = w, g \quad \textbf{A.13}$$

Heat Loss Source and Sink

$$HL_V + HL_c \quad \textbf{A.14}$$

Thermal Aquifer Source/Sink Terms

The aquifer source/sink term for water component is

$$\sum_{k=1}^{nf} \rho_w q_{wk} qa \quad \textbf{A.15}$$

And for energy

$$\sum_{k=1}^{nf} (HA_{CV} + HA_{CD})_k \quad \textbf{A.16}$$

Chemical Reaction and Interphase Mass Transfer Source/Sink Terms

The reaction source and sink for component i is:

$$V \sum_{k=1}^{nr} (s'_{ki} - s_{ki}) r_k \quad \textbf{A.17}$$

And the reaction source and sink term for energy

$$V\sum_{k=1}^{nr} H_{rk}\, r_k \qquad \textbf{A.18}$$

The discretized mass conservation equation is

$$\frac{\partial}{\partial t}\left[V_f\left(\rho_w S_w w_i + \rho_g S_g y_i\right) + V\varphi_v c_i\right] \qquad \textbf{A.19}$$

$$= \sum_{k=1}^{nf}\left[T_w\rho_w w_i \Delta\Phi_w + T_g\rho_g y_i \Delta\Phi_g\right] + V\sum_{k=1}^{nr}(s'_{ki} - s_{ki})r_k$$

$$+ \sum_{k=1}^{nf}\left[\phi D_{wi}\rho_w\, \Delta w_i + \phi D_{gi}\rho_g \Delta y_i\right] + \delta_{iw}\sum_{k=1}^{nf}\rho_w q_{wk} qa$$

$$+ \rho_w q_{wk} w_i + \rho_g q_{gk} y_i \quad [well\ layer\ k]$$

The energy conservation equation

$$\frac{\partial}{\partial t}\left[V_f\left(\rho_w S_w U_w + \rho_g S_g U_g\right) + V_v c_s U_s + (1-\varphi_V)U_r\right] = \qquad \textbf{A.20}$$

$$= \sum_{k=1}^{nf}\left[T_w\rho_w H_w \Delta\Phi_w + T_g\rho_g H_g \Delta\Phi_g\right] + V\sum_{k=1}^{nr} H_{rk}\, r_k + HL_V$$

$$+ HL_c + \sum_{k=1}^{nf} k\Delta T + \sum_{k=1}^{nf}(HA_{CV} + HA_{CD})_k \quad + \rho_w q_{wk} H_w$$

$$+ \rho_g q_{gk} H_g \quad [well\ layer\ k]$$

Boundary conditions at the wellbore can be defined as follows:

- Constant pressure $p_{wf}=p_{spec}$
- Constant water rate $\sum_{k=1}^{n_{lay}} q_{wk} = q_{spec}$
- Constant gas rate $\sum_{k=1}^{n_{lay}} q_{gk} = q_{spec}$

The discussed equations are solved simultaneously for each grid block along with the well equations. The time is discretized a s well. We have:

- 2 component conservation equation
- Energy conservation equation
- Phase constraint $S_w+S_g=1$

Equations are solved simultaneously, using Newton's method, in a generalized form which can handle many coupled equations. The equations that are summarized above are written in residual form as

$$R_i = [net\ inflow\ rate] + [net\ source\ and\ sink\ rate] - [rate\ of\ change\ of\ accumulation] \quad \textbf{A.21}$$

and the equation is solved when $R_i=0$. Evaluation of the residuals R_i amounts to calculating all the terms in the equations. The following calculations sequence is used:

1. Choose primary variables
2. K values
3. Remaining saturations and mole fractions
4. Densities, Enthalpies, internal energies
5. Reaction rates, Solid concentration, reaction source and sink terms
6. Porosity and accumulation terms
7. Relative permeabilities, viscosities, velocities, flow terms
8. Well rates and source and sink terms
9. R_i for n_{c+1} conservation equations and one phase constraint (when required)

If there is n_b active grid blocks and n_w open wells, then the total number of equations will be

$$N_{eq} = n_b(n_{eq}) + n_w \quad \textbf{A.22}$$

There are also N_{eq} primary variables. Let X_i represent all primary variables, with i=*1 to* N_{eq}. In general, each residual R_i could depend on each X_i, which is written as

$$R=R(X) \quad \textbf{A.23}$$

Where R and X are N_{eq} – length vectors. Advancing the solution over a time step consists of solving $R(X)=0$. This is accomplished using Newton's method, which is written as

$$X^{k+1} = X^k - [J^k]^{-1}R^k \quad \textbf{A.24}$$

Where J=dR/dx is the Jacobian Matrix of derivatives and k is the Newton's iteration number. The initial Xo is usually XN the solution, the solution to the previous time step. The iterative process is considered converged when both (X^{k+1} – X^k) and R are sufficiently small, at which time the solution at the current time is X^{N+1}=X^{K+1}

The entries in the Jacobian are

$$J_{ij} = \frac{\partial R_i}{\partial X_j} \quad \textbf{A.25}$$

In general, J has N_{eq}^2 entries, i=1:N_{eq}, j=1:N_{eq}

The non-zero Jacobian entries are estimated using numerical differentiation.

$$J_{ij} = \frac{R_i(X + \delta X_j) - R_i(X)}{\delta X_j} \quad \textbf{A.26}$$

where the sum X +δX represents the addition of ∂X to X_j while keeping the other X_m, m≠j, unchanged. when dXj is small this cordslope is a good approximation to the tangent slope$\partial R_i/\partial X_j$.

Treatment of gas hydrates

The conservation equation per gross volume of solid component i is:

$$\frac{d}{dt}[\varphi_V C_i] = \sum_{k=1}^{n_r} (S'_{ki} - S_{ki}) r_k \qquad \textbf{A.27}$$

where

φ_V – is the void porosity (ratio of void volume to gross volume)

C_i – is the concentration of component in void volume

S'_{ki}- is the product stoichiometric coefficient of reaction k

S_{ki}- is the reactant stoichiometric coefficient of reaction k

r_k- the rate of the reaction

This equation depends entirely on quantities local to the grid block, and so can be solved fully implicitly and simultaneously. This treatment of solid concentration allows the model to advance timesteps large enough that c_i and φ_f change significantly. It is not unusual for solid coke fuel to occupy 5 to 20 percent of the void pore volume. In these cases a very implicit and stable method is a requirement for the successful calculation of c_i and φ_f .

This treatment is complicated by the fact that fluid φ_f (used to calculate r_k) is a function of solid concentration c_i.

The following are the general steps taken in calculating the reaction rate rk and new solid concentration c_i:

1. Evaluate

$$\varphi_V = \varphi^o[1 + a(p - p^o) - b(T - T^o)]$$

Where

A – is the formation compressibility

B – is the formation thermal expansion coefficient

φ^o – is the porosity at porosity reference pressure

P and T – are the most recent values of pressure and temperature

2. Evaluate

$\varphi_V^N = \varphi_V[1 - \sum_{i=1} \frac{C_i^N}{\rho_{si}}]$

ρ_{si} – is the mole density of component I in the solid phase.

φ_V^N – is the combination of most recent p and T and N-level C_i^N

3. Replace the time derivative with a mass conserving discretization and solve the nonlinear equation

$R_i = \frac{\varphi_V C_i - \varphi_V^N C_i^N}{\Delta t} + \sum_{k=1}^{n_r}(S_{ki} - S'_{ki})r_k$=0

4. The solution of equation R_i=*0* for each solid set is accomplished via Newton's method

5. Make adjustments for preventing unphysical fluid porosity:

6. Using the new solid concentration ci, update the fluid porosity:

$$\varphi_f = \varphi_V[1 - F_{fluid} - \sum_{i=1} \frac{C_i}{\rho_{si}}]$$

For further use in evaluating accumulation terms.

APPENDIX B

Using the Fourier heat conduction partial differential equation of second order I derived the temperature distribution equation for this experiment.

$$T(R-r,h,t) =$$

$$= \mathrm{Tp} + \frac{\left(\frac{q_1 m_1 \beta_1}{V_1 C_P \rho_P} + \frac{q_2 m_2}{V_2 C_P \rho_P}\right) + \frac{\pi R^2 \Delta T_{sk}}{8 a_{gr} t_1} \exp\left(-\frac{R^2}{4 a_{gr} t}\right)}{1 + \frac{R\alpha}{2\alpha_{gr} a_p t} \exp\left(-\frac{R^2}{4 a_{gr} t}\right)} \exp\left(-\frac{(R-r)^2}{4 a_p t}\right) \qquad \textbf{B.1}$$

$$- \left(\frac{q_1 m_1 \beta_1}{V_1 C_P \rho_P} + \frac{q_2 m_2}{V_2 C_P \rho_P}\right) t_1$$

where a_p, a_{gr} – are the coefficients of thermal conductivity of the solution and soil, C_p - specific heat of solution, ρ_P - density of the solution, K - coefficient of thermal conductivity, m_1-mass of the gas released from hydrates decomposition per unit time, V_1 - volume of fluid in the borehole, β - the ratio of the coefficients of heat transfer of gas and liquid, q_1 - the amount of heat per unit volume of gas (heat of decomposition of hydrates transferred into the well stream gas evolved), m_2 - mass of evaporated methanol at given P and T, q_2 - latent heat of vaporization of methanol minus the specific heat of solution gas in methanol, V_2 - volume of liquid in contact with the gas, ΔT_{sk} – the temperature change in the time, T_P- temperature of the solution in the well during the 3d step, R – radius of the well, r – variable, the distance from the well axe to any point in the wellbore, d_{gr} – heat exchange coefficient of soil and wellbore, t_1 – time of gas hydrate decomposition of mass m_1, T - current time interval.